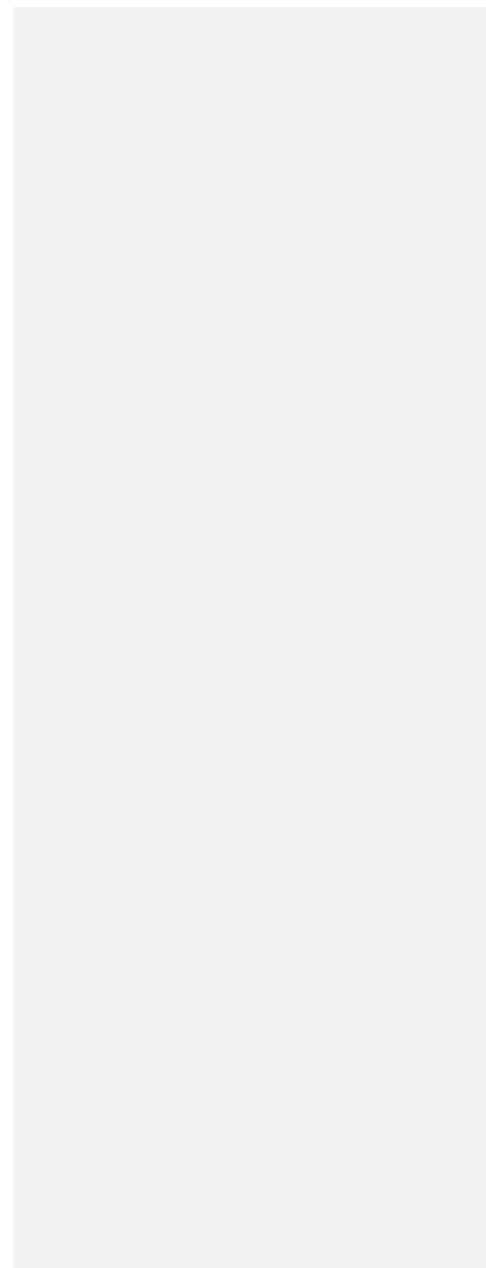


Thank you to the associate editor and the reviewers for your time with this manuscript review. We have
5 addressed all reviewer responses. Below we respond to each reviewers' points and note where relevant
changes in the manuscript have been made. We have also made some minor edits to the text for clarity.
The one large change we made was we added a figure showing VAF:PN (figure 7), similar to the
original VAF:POC figure (figure 6) . The track marked manuscript showing all updates follows the
response to reviewers' comments.



Response to Reviewer 1

Thank you for your comments, we appreciate your insight and we believe the paper has been strengthened and improved as a result. Below, we detail how we have updated our manuscript to address your comments. Actions taken are underlined

5

Comments on Bourne et al. paper

10 This paper conducts quantitative discussion on the relation between beam attenuation and settling particulate organic carbon / nitrogen / phosphate using Carbon Flux Explorer with time-series particle collector (CFE-Cals). In order to study the biological pump for quantifying CO₂ transport to the ocean interior, sediment trap experiment has been conducted all over the world ocean. However, moored or surface-tethered or even neutrally buoyant sediment trap has some specific disadvantages such as trapping efficiency and swimmer effect. In addition, it is hard to say that these “cost-performance” is high (need manpower and “ship time”). Nowadays, application of optical sensors such as transmissometer and backscatter meter to the study of marine particulate materials has been becoming more popular. However, although several scientists including one of co-
15 authors (Prof. Jim Bishop) have been making big efforts to calibrate optical data to actual POC and PIC flux, quantitative conversion of optical data to actual POC data is still on argument because optical observation spatiotemporally synchronized with particle observation has been difficult. Owing to development of CFE-Cals, this study has overcome this problem successfully, succeeding to Estapa et al. (2017). Thus, this paper is valuable for publication. However, I have some question and requests. Especially, discussion on comparison of previous reports is insufficient (explanation of previous papers is
20 ambiguous). I would like to ask authors to make medium revisions as follows.

Major Points

25 (I) I cannot follow how authors drew Fig.6, especially regression line or previous papers. Please explain how to estimate respective POC: VAF relations of Estapa et al (2017) and Alldredge (1998) (there is no direct description about this relation in the original paper unlike Bishop et al. 2016 (1.0/2.8)) in section 3.4 Comparison to previous studies (or in supplement).

30 *We have added in greater explanation in section 3.4 about how the Estapa et al. (2017) POC:VAF relationship was derived (page 12, line 5-8) and also how the Bishop (1978) and Alldredge (1998) volume:POC relationships were used to derive the POC:VAF relationships presented in Bishop et al. (2016) Added text: page 12 lines 15-32-page 13 line 2.*

35 (II) According to Figure A4 (Photograph of the surface-tethered BUOY-OSR) in Bishop et al. (2016), it seems that CFE-Cals was installed on the BUOY-OSR. I wonder if this data is not available. Although Bishop et al (2016) concluded that data obtained by BUOY-OSR is underestimated or sampling efficiency is low, if there is data, comparison of optical data and collected settling particle can be possible, POC/ATN relation can be proposed, and comparison of this data and present data can be possible.

40 *At the time of the 2013 experiments with the BUOY-OSR, we had hoped that analysis of the samples for P scaled by the Redfield ratio would yield carbon. We used Supor filters and analyzed the samples for phosphorous by ICP-MS with this in mind. However, we have shown in this paper that the regression of VA:PP when forced through zero ($r^2 < 0$) is worse than a random variation around a horizontal line; and only by selecting against the Anchovy pellet dominated sample do we get an r^2 of ~0.4. In contrast we have an $r^2 = .87$ for VA:POC or VA:PN for all samples. The material on Supor (polysulphone) filters cannot be analyzed for POC and PN. Given the fact that phosphorous to attenuation relationship is highly scattered and we do not have POC or PN data, we do not think the BUOY-OSR data are useful to include.*

45

We added a note regarding P analysis of BUOY-OSR samples on Page 3, lines 6 and 7.

(III) The configuration figure of CFE-Cals like Figure A1 of Bishop et al (2016) is great helpful for readers to understand CFE-Cals. I strongly recommend authors to add configuration figure of CFE-Cals to this paper.

We agree strongly with this reviewer that platform/sampler documentation should be provided. Figure 2 in the main text shows the sampler in its installed context and the flow path through sampler. In the appendix, we provide an image of the key element of the sampler. Figure A2 and its caption describe sampler and sampler flow logic. We have also included an instrument rendering from the CAD drawings to provide more detail of the overall configuration and the CFE-Cal sampler (supplemental figure A4).

(IV) When large amount of settling particle or gigantic settling particle cover over window, settling particle which settle down on covered window cannot be counted and amount of particles or PC must be underestimated with ATN. What do authors think about this?

This is an important consideration.

As light is reduced exponentially as it passes through particles, as long as the overlapping particles do not 100% obscure the transmitted light, attenuation affects are additive. In our analysis, the transmitted light even in the presence of multiple overlaid large aggregates, never went to zero (in other words, attenuation was never saturating, Bishop et al., 2016). Therefore, overlapping was not an issue in this study.

We added a discussion of this on page 4, line 30 to page 5 line 2.

Minor Points

(1) Page 1 Line 12 (P1L12) Why did not authors measure Ca with ICPMS? Because Bishop (co-author) reported that “we have no data on the conversion of PIC(POL) to PIC(flux)” in his previous paper (Bishop et al. 2016).

The VA:PP,PN,POC calibration was the priority for this paper and required by our funding. We did measure Ca with the ICPMS for the samples. As the filters had large amounts of residual sea salt, the separation of the non-salt Ca requires very high accuracy and a separate protocol. We are still working on this and the analysis of the cross-polarized light imagery.

We do have an accurate and physically based measure of particle birefringence (cross polarized photon yield), which is discussed by Bishop et al., (2016). When a calibration becomes available, all previous results can be translated into units of PIC.

We have made a note of this on page 4 lines 12-14.

(2) P5L14 Please explain why Fluorinet (3M) was selected as initial liquid.

Fluorinet was selected as it is clear (necessary as there was an optical encoder in the pressure compensated chamber), low viscosity (for motor immersion) and inert (necessary as there were electronics in the chamber).

Added discussion to page 5 line 25-27

(3) P5L16 Please explain how to rotate the sample selector rotator (is there motor and gear?)?

There is a motor with a planetary gear set whose output turns the sampler (2842S024C; Faulhaber Group, Micromo, Florida). An optical encoder provides feedback as to the proper location for the desired sampling bottle. Included in text.

Added details on page 5, lines 22-27.

(4) P9L20 Insert “(2008)” after “Lamborg et al.”

We fixed this.

(5) P10L30 Description “(data for regression in Table S1)” should be placed between “this study” and “vs”.

We moved this as suggested.

(6) P14L18 (reference) C.H.Lamborg => Lamborg, C. H.

We fixed this as suggested.

(7) Table 1 (1) What does asterisk (*) of some filters mean? Please explain.

The Asterix indicates the sample is a process blank. We note this in the figure caption.

(8) I think information of “tilt” is important. How about touching upon information of “tilt” when sampling briefly in table caption or in appropriate place in the text?

We added a figure into the appendix (A2) depicting tilt over time, similar to the figure in Bishop et al. (2016). We note that although tilt has negligible effect on particle collection efficiency, our requirement for the minimization of tilt is to facilitate even particle distributions on the sample stage. Added mention of tilt page 5, lines 5 and 6.

(9) Fig. 6 (1) Please explain difference between left figure and right figures. (2) Please explain “Estapa 2017” blue data and “Estapa 150 m” light blue data (150, 300, 500m data set and 150 m data, respectively?) (3) Blue color and light blue color are used not only for different regression lines (forced through zero intercept and allowing for an intercept), but also for different data set (150 m data only and all 150, 300, 500 m data?). This is confusable. Please change color set.

We reworded the figure caption as shown below.

Regressions of ATN-POC ($\text{mATN-cm}^2 \text{cm}^2 \text{d}^{-1}$) to POC ($\text{mmol C m}^2 \text{d}^{-1}$) for this study (orange line; $y = 1.03x$, $R^2=0.874$), Estapa et al. (2017, blue, $y = 1.56x + 0.434$, $R^2 = 0.632$; light blue line, $y = 2.191x$, $R^2 = 0.47$). Bishop et al. 2016 estimated slope (green line) is 0.357 (1.0/2.8). Alldredge (1998) estimated slope (purple line) = 6.25. As this study's calibration is created using samples collected at 150m, we separate out Estapa's (2017) data point collected in 150m by marking them in light blue for comparison. (A) shows the entire range of VAF and POC flux from this study. (B) expanded graph near the origin ($x < 3 \text{ mmol C m}^2 \text{d}^{-1}$) showing the range of Estapa et al. (2017) data.

(10)Table S2 (1) No description about Table S2 (2) More detail explanation about respective column in caption

We added a description of Table S2 in the caption. Table S2 contains the volume attenuation flux and the POC data for all the samples shown in figure 6. It also notes the CFE-Cal each sample was collected with, the dive number, the bottle number and the length of time the sample was collected over. Table S2 has been modified.

5

(11)References There are many mistakes and different description (e.g. Deep. Res., K.O Buesseler <=> Buesseler, K.O.). Please check format.

10 *We fixed all references*

Author response to referee 2.

Thank you for your review. We appreciate your insight and we believe the paper has been strengthened and improved as a result. Below, we detail how we have updated our manuscript to address your comments. Specific actions are underlined

5 SUMMARY In this manuscript the authors address a current critical research field aiming at better estimating the Biological
Carbon Pump (BCP) in the ocean by the use of autonomous in situ floats. These devices allow particle flux observations at
very high spatio-temporal resolutions essential to capture the rapid ecological changes responsible in a large part for the BCP
10 efficiency variations. In particular, this study targets a calibration between a proxy of particle concentrations in the water
column, the volume-attenuance (VA) measured with a Lagrangian float-deployed imaging sediment trap, the Carbon Flux
Explorer (CFE), and particle bulk chemical composition in Particulate Organic Carbon (POC), Particulate Nitrogen (PN) and
Particulate Phosphorus (PP) measured on the same particles previously imaged and collected with a novel particle sampler
15 added to the CFE (the whole instrument being named CFE-Cal). The ultimate goal of this calibration is an accurate estimation
of element fluxes directly from particle imaging which thus would offer large potential in term of flux data collection which
are still today and despite intensive efforts poorly spatially and temporally resolved. After detailing thoroughly the material
and methods employed for particle imaging, collection and analyses the authors present results from 15 deployments of the
CFE-Cal which lasted 18 to 24 hours near 150 m depth in four different locations in the California Current system selected for
20 their contrasting primary productivity features. Results show good correlations between particle content in C and N (but not
P) and VA, promising perspectives of using this autonomous in situ imaging to estimate the fluxes of these elements. Each
result is discussed (Results and Discussion grouped in the same section) and focus is put on results not meeting authors
expectations or not agreeing with the literature. For the results that deviate from expectations, the authors suggest possible
explanations from either material malfunctions or the characteristics inherent to the different environment sampled.

25 GENERAL COMMENTS AND RECOMMENDATIONS This manuscript is well-written and leaves the reader with the
general impression of a solid piece of work. Each section is correctly articulated and information are in general presented
where they are expected. Overall, the figures and table shown are clear and deliver well the message intended. The objective
tackled here is with no doubt one of the main current and future challenges in BCP research studies (converting particle flux
from in situ imaging to biogeochemical fluxes) and I am always pleased to read about work that try to push further our methods
30 to measure these complex and very dynamic ecological processes that drive the BCP with technical innovations. Even if not
realising a major advance in the field and presenting results that could be argued, especially in term of potential bias, dataset
size and finding significance this study is worthy being published in BG because it is an attempt to a step forward and will
certainly interest the research community working on ocean particle fluxes. However, even if I acknowledge the work done,
its quality and how it is presented I have some concerns about this manuscript that lie mostly on a lack of details about the
35 limitations of the method employed, that also reflect in the results, discussion and the general conclusion made by the authors.

- (1) To obtain a good conversion from particle images to POC, PN and PP content, two key parameters have to be
carefully considered: (1) the conversion from particle 2D images obtained by the CFE to their 3D volume
(detailed in Bishop et al., 2016).
40 Briefly, in Bishop et al. (2016), aggregate (including those of phytodetrital and fecal origin) volume was
inferred from cross sectional area converted to equivalent circular diameter and then to volume using an
empirical relationship between aggregate thickness and their equivalent circular diameter reported in Bishop et
al. (1978); (2) The conversion from particle volume to their chemical content. For that Bishop et al. (2016)
45 used a published value for aggregate dry-weight density (0.087 g cm^{-3} ; Bishop et al., 1978), and an estimated
fraction of organic matter of 60 % in total dry weight. Finally, Bishop et al. (2016) uses an OM:C ratio of 1.88
to convert the estimated OM weight to POC.

*Bishop et al. (2016) had to estimate POC in the CFE imagery as no calibration samples for POC and PN were collected.
In this study, we were able to collect corresponding POC samples using the two CFE-Cals. We therefore did not need to
do any conversions of 2D images to 3D volumes to estimate carbon as was done in Bishop et al. (2016).*

In this paper, we report that the estimate of VA:POC ratio estimated by Bishop et al. using a 2D to 3D volume conversion formula and information on particle density and carbon contents from Bishop et al. (1978), differed by a factor of 3 from the calibration presented here. This is shown in figure 6. We've added a more detailed explanation of this on page 12 line 15 to page 6 line 6.

(II) The authors highlighted clearly the problem of using these literature-based calibration factors as they are often applicable only in the limited spatio-temporal context of their formulation. But I hardly understand the aim of the present calibration if it is not to finally succeed at reconstructing the flux from images alone and from a large range of environment and ecosystem structures. From the way it is currently presented, the manuscript suggests that the authors are trying to establish a library of relationships between VA and C, N, P contents. If it is the case it should be clearly stated.

Our goal is to reconstruct flux from images. In the future, using the CFE-Cals to collect samples from more regions will make the calibration more robust and widely applicable. We emphasized these goals more clearly in the conclusion. See page 13: lines 18-32 and Page 14 lines 1 to 10.

(III) I would have found very interesting to see in the discussion and conclusion sections some perspectives on how to improve the calibration presented here. In particular, the combined acquisition of particle images and measurements of POC, PN and PP done here offers the great opportunity of estimating the quality of a traditional flux reconstruction (i.e. by inferring its value from the images using published volume to organic contents conversion factors as done before) by comparing it to the real values measured here (as explored in Estapa et al., 2017). I assume that the final goal is to estimate the POC flux from images alone and much work is yet to be done by the community to understand how to translate small differences in image detection to potentially large differences in chemical contents.

A comparison between the calibration method developed here and other methods that try to convert images to elemental fluxes should have been made. The use of Polyacrylamide or Cryogels sediment traps to collect particles and then use image analysis and published values of organic content to convert the images to fluxes is a very close approach to this study. The major advance that the present work could have brought is by extending the use of particle images to push further the estimation of their organic content from the image analysis. It is a bit disappointing to finally realise that this study has the great potential of presenting both the images and the "true" values of their content usable to further our understanding of observed discrepancies but that unfortunately this opportunity was not seized by the authors.

We respond to the suggestion that fluxes should be estimated based on previously published particle volume to carbon relationships as done previously in gel trap studies in response to point B below.

In the future, a study of gel trap samples and CFE imagery needs to be done on the same platform and same time and with careful attention to the photography and illumination of gel trap samples. We'd love to facilitate such a comparison in the future but this activity is beyond the scope of this paper. The best same place, same platform, same time study is that of Estapa et al. (2017) who used 2D size distributions in gel trap samples to estimate carbon. They did not extend the analysis of gel trap imagery to attenuation units. The main requirement is that the illumination source intensity (without particles present in the gel) must be mapped precisely as we do with the CFE. Variations in gel homogeneity and thickness degrade particle detection.

Also, the limited number of results obtained due to device malfunction or inherent to the properties of the particle flux collected (i.e. presence of swimmers), or the corrections of POC, PN and PP values obtained from the CFE004 dives due to a discrepancy between images and sampling, should have led the authors to much more caution in their conclusion.

Instead, the authors claim "strong calibrations" between the VA and POC-PN contents for a dataset on which many values

have been removed or multiplied by an empirically-determined factor; in this case the 1.45 times factor representing the difference of abundance of ovoid pellets in the sampler and from the images.

We've changed "strong calibrations" to "well-correlated. In the detailed comments section we respond to point 19 on removing the C/N points and point 16 on the 1.45 empirical factor.

Based on all these general remarks, I still recommend this article for publication in BG but after significant changes have been made to the Results, Discussion and Conclusion sections and substantial evidences provided where required.

In particular, I strongly advise the authors to focus on the general issues mentioned above and summarised as follows:

(A) Add to the manuscript a comparison with other techniques of image conversion to biogeochemical fluxes (e.g. gel sediment trap analyses).

This recommendation is addressed in (III) above. This is worth-while to do when such particle collections are made simultaneously, ideally on the same platform. We do not agree that comparison to gel trap sample size distribution analysis should be brought into the present discussion.

(B) Use the dataset presented to explore further the known discrepancies between image analysis and inferred organic content. The authors could investigate if a reconstruction of the fluxes measured by the sampler here would be feasible by using the corresponding images and by applying various volume to chemical content relationships to the different particle types identified (e.g. different relationships for fecal pellets, marine snow, etc.). New insights informing on why we struggle at inferring the flux from images would certainly increase significantly the impact that this manuscript will have on the research community.

In regards to reconstructing fluxes from published volume to carbon rations, we do compare our VAF:POC to ratios derived using previously published volume to carbon ratios (Alldredge, 1998 and Bishop et al., 1978) reported in Bishop et al. (2016). Aggregates are a component of flux at all our locations. The typical volume to chemical content relationship for aggregates is from Alldredge (1998). This has been used in both gel trap imagery (Ebersbach and Trull, 2008; Ebersbach et al., 2011) and aggregates collected then imaged using Marine Snow Catchers (Riley et al., 2012; Baker et al., 2017).

We've provided a more detailed description of the Alldredge method and why our calibrated relationship of VAF:POC is not consistent with it on page 12 lines 15 to page 13 line 6.

The discrepancy likely stems from the fact that aggregates are collected and photographed using different methodologies which may affect their volumes. The Alldredge aggregates are photographed underwater in the plane parallel to the particle sinking direction, whereas the aggregates in the CFE are photographed perpendicular to their sinking direction after the aggregates have settled onto the glass stage. Though settling is very gentle, a 3D particle landing on a 2D surface will have some degree of compaction. Also, the aggregates from the Alldredge (1998) study were collected in the euphotic zone whereas our samples are from the mesopelagic.

As we know there are methodological differences between how fluxes are reconstructed from images in gel trap studies and how images are collected using the CFE, and we further know from Bishop et al. (2016) that the relationship of VA:POC derived using the Alldredge (1998) and Bishop et al. (1978) relationships of VAF to POC differ from the relationship directly calibrated in this study, we do not believe it would be useful to add a flux reconstruction based on particle volumes here. We do believe in the future it would be useful to do an intercalibration as mentioned above.

(C) Depending on the modifications made after (1) and (2), moderate if needed the stated significance of the results and discuss it more objectively and into details. Especially, the term "strong correlation" can hardly be used with such confidence

knowing that the dataset has been trimmed and partly multiplied by an empirically-determined factor, and that authors seem themselves unsure about potential contaminations of their samples.

We've modified our conclusion section to stress that these are initial calibration results, and that more work is necessary to make the calibration more robust. We've also removed the term strong correlation, replacing it with well correlated. These points are addressed in further below in the detailed comments section.

Additionally, below are more detailed comments on the manuscript including technical and typographical corrections that will need particular attention before publication. I advise the authors to give a special attention to the four questions/comments below marked with an asterisk (*) as their response should influence the final decision for publication.

DETAILED COMMENTS

- 1) Page 1, Line 17: please add to the R^2 the size of the sample included in the fit (n) and the p-value.

We have added in the n and p values.

- 2) Same line: "...was not sensitive to environment or classes of particles sampled." I assume this statement is used as a proof of applicability of the current calibration to many different ecological contexts. But, it could also suggest that the environment where the deployments were made was not contrasted enough for this calibration.

Figure 3 and 5 were intended to contrast particle size distributions and classes found at each location. We will add clarifications of details of the variability of the environments and size distribution at each collection site. We have changed Page 1 line 19 to read "was not sensitive to particle size classes or the contrasting environments encountered."

- 3) Page 1, line 21: a space is missing between "Approximately" and "10".

This has been fixed.

- 4) Page 3, line 11: change "our 2.8 conversion factor" to "the 2.8 conversion factor obtained by Bishop et al. (2016)". I understand it is the same team but "our" would mean version Discussion paper a factor inferred in the current study and it is not the case.

This was changed.

- 5) Page 4, line 9: the glass stage appears quite small and subjected to overload if a single cm-sized particle (or a few mm-sized particles) happened to enter in the trap. What is the diameter of the opening?

We added in the diameter of the funnel opening (page 4 line 9). We address sample overloading in the response to point (6).

- 6) Page 4, line 13: The time of ~25 min seems critical. Is there a threshold at which volume attenuation can be biased by particle overload (particles accumulating over previously deposited particles on the stage)? How did the author choose this time and the time of ~1.8h mentioned below (line 14) as it seems dependent upon the amplitude of the particle flux at the time and depth of the deployment?

The times were chosen to allow for high temporal resolution of flux and since we were not power limited (CFE can operate for 8 months at hourly frequency) we chose by default cleaning times to be the same as times used by Bishop et al. (2016).

We have added this discussion to page 4 line 19.

5 *Overlapping particles do not bias attenuation flux as their contributions are additive. (see discussion in Bishop et al., 2016 and also our response to Reviewer 1 on this point). Implied is the question of whether or not attenuation is saturated (e.g. transmission is 0). The highest fluxes recorded by the CFE were those from January 2013 discussed in Bishop (2016). Even at this high rate of flux, attenuation was not saturated. We have not seen evidence of saturating attenuation in our images from CCE-LTER.*

10 *We have added a discussion of this on page 4 line 30 to page 5 line 2.*

7) Page 6, line 5: do particles larger than the size limit of 3 mm can get stuck inside the openings?

15 *Aggregates and rare gelatinous organisms larger than 3 mm do not get stuck. In one of our 23 deployments, a larval crab became stuck in the stage area and had to be removed after recovery. We added a discussion of this on page 6 line 15-17.*

8) Page 6, lines 7-8: I assume the CFE-Cal has not yet been used for trace metal studies then (this intended use is mentioned above in the manuscript)?

20 *Yes, we designed the CFE-Cal so that in future it can be used for trace metal studies. More refinement is required. No change to text.*

9) Page 7, line 3: peri slides. Please correct.

25 *This was fixed.*

10) Page 7, line 16 and below: why giving results in the Material and Methods section?

This has been moved to the results section.

30 11) * Page 7, lines 19-22: this will need clarification as it seems to be a very serious issue. How could the process blanks be higher than the samples themselves even in case of accidental collection or contamination? Over the 6 replicates of process blanks, how many were contaminated? How did the authors deal with this issue as blanks have to be subtracted from sample values? Are the negative values on Fig. 5A a result of this correction?

35 *We have clarified the discussion of blanks on page 9 lines 9-18.*

40 *Process blanks were subtracted from sample values, as shown in equation 1. The negative value was a result of this correction. As there were only 5 QMA process blanks, an average of the five was used to blank correct POC and PN. This drove one POC and one PN sample from Location 3 negative, though not negative within error (errors calculated following equation 2). Fluxes at location 3 were very low - an order of magnitude lower than samples collected in other regions.*

45 *All process blanks and replication (if process blank analysis was replicated, average of the analyses was taken before calculating overall process blank average of the 5 unique samples) had some level of carbon and nitrogen which is attributed to collection either during deployment or sample processing, none were excluded from the calculation.*

12) Page 7, lines 24-25: "... which we assume is based on sample heterogeneity". Do the authors have evidence to support this assumption?

5 *The samples were punched from the filter as described in the methods. We retrieve punches evenly distributed across the filter, but inevitably as there are discrete particles on the filter, there is some heterogeneity between the sub-samples. The sample is not homogenized and then sub-sampled. As this same process is done for every sample, we applied the RSD in the error calculation. We've more clearly explained this on page 9 line 20-23. Figure A5 depicts particles dispersed across filters.*

10 13) Page 8, lines 24-25: please mention what would have been the total number of samples in case of no malfunction or swimmers and give a percentage of "fail". My point is that it is hard to estimate the robustness of the CFE-Cal without a proper estimation of its percentage of fail (how many successful dives/samples over the total number intended?).

We've added a discussion of this to page 8 line 21 to page 9 line 2.

15 14) Page 8, line 27: this is not really a measure of "collection efficiency" (only assumed) but more a measure of transfer efficiency between the imaging stage and the bottles.

We changed the Heading 3.2 (page 9, line 26) to Transfer Efficiency.

20 15) Page 8, line 29: "...close...", please give a precise number.

Updated to give percentage on page 8 line 29-30

25 *CFE-Cal2 collected close to the same number of particles in the sampler as were imaged (on average, there was less than a 9% difference between particles imaged and particles collected on the filter, there was not exclusively more in either the CFE images or on the filters as there was for CFE4, see figure 4).*

30 16) * Page 8 line 30: again this is a very worrying result that needs more investigation as it suggests a real issue with the collection and/or transfer method employed.

* Page 9, line 1 and lines 3-4: the authors first state that they do not fully understand the issue and then claim to have addressed the problem by solving a software issue. Please bring clarification on this.

We added clarification of the software issue and how it was addressed on page 9 line 31 to page 10 line 6.

35 *We do believe that our empirical factor does correctly address the CFE-Cal4 calibration data. We note on page 9 line 19 to 24, that even removing all the CFE-Cal4 data with the collection issue, the VA:POC and VA:PN slope changes less than 5%:*

We've added the following discussion to page 11 lines 19-24:

40 *As mentioned earlier, we found that CFE4 collected 1.45 times more ovoid pellets on the filters than were imaged due to a sampling issue and that we therefore divided the CFE4 POC and PN samples for location 1, 2 and 3 by this empirically derived factor. This affected 6 samples in the POC and PN regressions (see table S1). We note that if instead of applying this empirical factor, these samples are removed from the regression, the VA: POC and VA:PN slopes both change less than 5%. The slopes (number of samples, R² and p value in parenthesis) change to 10.6 x 10³ (n=8, R²=0.93, p<0.001) and 10.4 x 10⁴ (n=9, R²=0.91, p<0.001). Using these data which have been corrected using the empirical factor therefore affects the overall regression very little.*

45 17) Page 9, line 12: what does this time of 2 minutes sample collection time refer to? (how is it different to the ~25 min imaging sequential time?). Is it the duration of particle transfer to the bottles?

This is the duration of particle transfer time during a cleaning cycle. A cleaning cycle takes 2 minutes to complete. The 25-minute timing is the time interval between successive image sets after a cleaning cycle. We've clarified this on page 10 line 14.

5 18) Page 9, line 17: please add the sample size (n) and p-values for each regression fits. Page 9, line 17-25: being "not typical of sinking particles" is certainly not a valid reason to exclude these values from the dataset. Authors are required to provide valid reasons here (e.g. why these C/N ratios would make these particles not wanted in this dataset?).

We added n and p values page 10 lines 19-20

10 *We added the regression values for if the high C/N particles are included on page 11 line 1. We also add more of a discussion of the reasoning behind the C/N exclusion, as discussed below.*

15 19) * Page 9, lines 26-32: again this is a very serious issue. If the sampler building material is potentially responsible for contaminating the samples, how can the authors be confident that not all their POC and PN values are biased by chemicals leaked from this 3D printed part?

We've added more discussion of this from page 10 line 27, to page 11 line 2.

20 *PN values would not be biased by chemicals from the 3D printed part as the material contains no nitrogen. All the other samples have C/N values typical of sinking particles.*

20) Page 10, lines 1-4: this also seems to be pure speculation without any evidence of TEP presence in samples.

25 *This was a hypothesis which we removed.*

30 21) Page 10, line 8: if I understand well, the objective of this calibration is to ultimately allow an estimation of biogeochemical fluxes from in situ imaging that could be applied to the largest range of particle types and flux amplitude. It seems very contradictory then to remove particles from the dataset because they are inherently different from the rest of the flux to improve the goodness of the fit. This is very troubling as it suggests that the authors don't fully comprehend their ultimate goal here. Page 10, line 10-13: this is precisely why it seems so hard to reconstruct a biogeochemical flux from images alone. I strongly suggest that the authors use this example to illustrate the difficulty of meeting the challenge addressed here and impartially discuss their results following the approach of reconstructing the flux from its various particle types having contrasted chemical contents (see general remarks above).

35 *In the lines you mention, we discuss how the high P content of anchovy fecal pellets, combined with the fast sinking rates, led to phosphorous loadings far higher than the other samples. Though the ultimate goal is to allow an estimation of biogeochemical fluxes based on image analysis, we concluded that we cannot predict particulate phosphorous flux based on VAF, precisely because of the highly heterogeneous nature of phosphorous in particles, such as the anchovy pellet. In other words, as P is highly labile, we found it was impossible to estimate PP based on in-situ imaging. Our intent was to show that even when eliminating that particular point, the relationship between PP and VAF was still far less robust than that of POC or PN.*

40 *We've removed figure 5 part d, as well as clarified our conclusions on page 11 lines 8 through 17 to make this more clear.*

45 22) Page 11, line 26: please remove "strong" as it does not seem appropriate. Provide n and p-values.

50 *We changed strong to well-correlated. N and p values have been added.*

23) Page 11, lines 26-27: " that apply over a wide range of environments". This statement could be made with confidence only if the deployments were made in different oceanic regions, seasons and water column layers. It appears too early at this stage to claim this. Page 11, line 31: "... insensitive to particle classes dominating export". This is not true and is directly contradicted by previous findings shown in this manuscript (see observations made by the authors about the anchovy fecal pellet flux). Please amend as required.

We changed the wording in the conclusion to describe the different environments encountered.

24) Page 12, lines 5-8: this is confusing and again suggests contradictory intentions of the authors. It is still unclear at this very end of the manuscript if the authors intend to establish a library of VA:element fluxes relationships for each environment and ecological settings sampled (the use of one specific slope would then be reusable to infer the biogeochemical fluxes from images taken in the corresponding region, time of the year and depth), or if they intend to find a general relationship usable in many oceanic regions, environments and ecosystem structures. In both cases, an extensive work remains to be done and it should be clearly stated.

Our results are a first step towards expanding the range of particle flux that may be retrieved through optical methods. We've rephrased the conclusion to make this clearer. We also renamed the section "Conclusions and future development", rather than just conclusions. We also stressed multiple times that these are initial results, and more work is necessary to make the calibration more robust.

Carbon Flux Explorer Optical Assessment of C, N and P Fluxes

Hannah L. Bourne¹, James K.B. Bishop^{1,2}, Todd J. Wood², Timothy J. Loew² and Yizhuang Liu¹

5 ¹Department of Earth and Planetary Sciences, University of California, Berkeley, Berkeley, 94720, USA

²Lawrence Berkeley National Laboratory, Berkeley, 94720, USA

Correspondence to: H. L. Bourne (hbourn@berkeley.edu)

Abstract. The magnitude and controls of particulate carbon exported from surface waters and its remineralization at depth are poorly **constrained**. The Carbon Flux Explorer (CFE), a Lagrangian float-deployed imaging sediment trap, has been designed to optically measure the hourly variations of particle flux to kilometer depths for months to seasons while relaying data in near-real time to shore via satellite without attending ships. The main optical proxy of particle load recorded by the CFE, volume-attenuance (VA; units of mATN-cm²), while rigorously defined and highly precise, has not been robustly calibrated in terms of particulate organic carbon (POC), nitrogen (PN), and phosphorus (PP). In this study, a novel 3D printed particle sampler using cutting edge additive manufacturing was developed and integrated with the CFE. Two such modified floats (CFE-Cals) were deployed a total of 15 times for 18-24-hour periods to gain calibration imagery and samples at depths near 150 meters in four contrasting productivity environments during the June 2017 California Current Ecosystem – Long Term Ecological Research (LTER) process study. Regression slopes for VA: POC and VA:PN (units mATN-cm²: mmol; R², **n**, **p**-value in parentheses) were 1.01×10^{-4} (0.86, 12, <0.001), 1.01×10^{-5} (0.86, 15, <0.001) respectively and was not sensitive to **particle size classes or the contrasting environments encountered**. PP was not well correlated with VA **reflecting the high** **libability of P relative to C and N**. **The VAF-POC flux calibration is compared to previous estimates.**

1 Introduction

Marine phytoplankton account for about half (or 50 Pg C y⁻¹) of global primary productivity and live for one week on average before being consumed by zooplankton (Falkowski et al., 1998). Approximately 10 Pg C y⁻¹ is exported from the surface layer as sinking aggregates containing both particulate organic and inorganic carbon (POC and PIC). The carbon that reaches the deep ocean remains isolated from the atmosphere for centuries. This process, the “biological carbon pump” (BCP), is a fundamental player in the global carbon cycle, **yet** the stability of the BCP and its future in the face of climate forced circulation changes and ocean acidification are currently unknown. **Recent** studies have noted discrepancies in reconciling meso- and bathypelagic activity with current euphotic zone flux estimates (Banse, 2013; Burd et al., 2010; Ebersbach et al., 2011; Passow, 2012; Stanley et al., 2012). **Furthermore**, estimates of carbon flux out of the euphotic zone range **widely** from 6 to 12 Pg C y⁻¹ (Dunne et al., 2005; Siegel et al., 2014; Yao and Schlitzer, 2013). More traditional methods of measuring particle flux in the ocean rely on sediment traps or geochemical sampling that require ship time (Buesseler et al., 2007). As ship time is expensive

Deleted: known

Deleted: 10.07

Deleted: 3

Deleted: 2

Deleted: 3

Deleted: 10.0

Deleted: 5

Deleted: 4

Deleted: 7

Deleted: 5

Deleted: 6

Deleted: environment or classes of particles sampled

Deleted: .

Deleted: T

Deleted: A number of

Deleted: r

Deleted: Recent

both in terms of funding and labor, flux measurements conducted this way are temporally and spatially limited. In recent years, there have been a number of developments towards autonomous instruments capable of measuring particle flux [using optical methods](#) (Bishop et al., 2004, 2016; Briggs et al., 2011; Estapa et al., 2013, 2017).

The attenuation of light by particles has long been used by oceanographers as a measurement of particle concentration in the ocean water column, beginning with development of underwater transmissometers in the early 1970s (Zaneveld, 1973). Transmissometer beam attenuation coefficient (at 660 or 650 nm) has been shown to strongly correlate with measurements of particulate organic carbon (POC) concentration in the water column (Bishop et al., 1999; Bishop and Wood, 2008; Boss et al., 2015; Gardner et al., 2000). Transmissometers were first deployed vertically mounted on Lagrangian profiling floats (called the Carbon Explorers, CEs) in 2001 in the North Pacific (Bishop et al., 2002). These deployments revealed a systematic loss of transmission as the CEs drifted at depth between profiles. A trend of increasing transmission was seen in the deepest 200-300 m as the CEs rose from 1000 m to the surface, implying that particles had accumulated on the upward looking transmissometer window during drift and were being washed off during initial stages of profiling. CE's deployed in the Southern Ocean in 2002 were modified to measure transmittance before and after exhaust flow from the float's CTD pump was used to clean particles off the transmissometer window during drift and thus a Carbon Flux Index (CFI) was derived as a systematic measure of particle flux over time (Bishop et al., 2004, [Bishop and Wood, 2009](#)). Estapa et al. (2017) advanced the quantitative use of float-deployed transmissometers to estimate particulate carbon flux and more properly derived a flux proxy based on beam attenuation change over the 1-2 days that their neutrally buoyant traps drifted at depth. The Estapa et al. (2017) method does not involve optics flushing.

The Carbon Flux Explorer (CFE), which combines an imaging Optical Sedimentation Recorder (OSR) and profiling Sounding Ocean Lagrangian Observer (SOLO) float, periodically images particles as they accumulate on a glass sample stage. It thus builds upon the concept of optically measuring particle flux by quantifying particle attenuation at each pixel (Bishop et al., 2016). ~~The imaging instrument also fully resolves particle classes from 20 μm to cm scale. As transmissometer beam attenuation coefficient was found to be highly correlated to POC concentration within the upper 1000 m of the ocean, a reasonable assertion would be that light attenuation of particles integrated across an image (volume attenuation) would also be highly correlated to POC load. Image attenuation (ATN) is the combined effect of both light scattering loss and light absorption by particles, it is calculated by taking the $-\log_{10}$ of a transmitted light image normalized by an *in-situ* blank composite image of the particle free sample stage (Bishop et al., 2016). Integration of ATN across the sample stage area yields Volume Attenuance (VA, units: $\text{mATN}\cdot\text{cm}^2$), a measure of particle load. Normalizing by trap opening and time deployed yields Volume Attenuance Flux (VAF, units: $\text{mATN}\cdot\text{cm}^2\text{ cm}^2\text{ d}^{-1}$).~~

Successful calibration of VAF in carbon units would allow for far greater temporal, and spatial resolution of carbon export than possible with ships and thus inform current models of biological carbon flux as CFEs have the capability of observing hourly variation of particle flux at depth for months to seasons (Bishop et al., 2016). An earlier attempt to calibrate the CFE in

Deleted: float

Deleted: ; Bishop and Wood, 2009

2013 used a surface tethered OSR and sampler (shown in McDonnell et al., 2015 Fig. 3F). This method failed as it was discovered that simultaneously deployed surface-tethered OSRs and Lagrangian CFEs collected far different particle types, size distributions, and quantities of material (Bishop et al., 2016). The surface-tethered OSR was biased low ~~due to “baffle bounce”~~ as much as a factor of 20 and collected almost no material larger than 1.5 mm; ~~in other words, the larger aggregates~~ encounter the cm sized openings of the ~~tethered~~ trap in a near horizontal trajectory and thus bounce back into the flow rather than accumulating in the trap. ~~The samples from the surface tethered OSR were analyzed for phosphorus as a POC proxy, but this approach was not productive as will be shown below.~~ Lacking ~~appropriate~~ calibration samples, Bishop et al. (2016) utilized aggregate size – POC weight estimates from Bishop et al. (1978) to derive a factor of 2.8 for scaling VAF (mATN-cm² cm⁻² d⁻¹) to POC flux (mmol C m⁻² d⁻¹); they note that applying the Alldredge (1998) volume-POC formula for marine snow particles collected by scuba in shallow waters yielded a conversion factor of 0.16, about 17 times smaller than the estimate based on Bishop et al. (1978).

Deleted: by

Deleted: words

Deleted: .

Deleted: These

Estapa et al. (2017) working in oligotrophic waters near Bermuda compared sediment trap POC flux with transmissometer (650 nm) attenuation drift; conversion of their results (Fig. 7 in Estapa et al., 2017) ~~in our units of VAF: POC yielded factors ranging from 0.46 to 0.74, four to six times lower than the 2.8 conversion factor. We note that a log₁₀ to ln conversion error in~~ Estapa et al., 2017 implied a greater difference. ~~Multiple optical reasons for differences may include: (1) beam collimation (CFE uses a diffuse LED light source and camera (Bishop et al. 2016) whereas transmissometers are highly collimated but can vary a factor of two in sensitivity based on differences of beam geometry and receiver acceptance angle (Bishop and Wood, 2008; Estapa et al., 2017), (2) effects of particle size distribution on attenuation, (3) wavelength dependence of attenuation (CFE uses the green image plane (~550 nm) vs. (650 nm) red transmissometer), and (4) stray light. Estapa assumed 100% collection efficiency of particles on the vertically facing transmissometer window and zero contribution of optics biofouling to her measurements. The difference in slopes may be also method dependent as Estapa et al. (2017) analyzed only the particulate carbon in 350 µm screened material from the sediment traps whereas the Bishop et al. (2016) factor includes larger aggregates up to cm size.~~

Deleted: (at 650 nm)

Deleted: (in our units of VAF: POC)

Deleted: our

Deleted: (

Formatted: Font color: Text 1, Subscript

Deleted:)

Deleted: (650 nm)

Deleted: neutrally buoyant

Deleted: is based on

Given ~~the~~ finding of a factor of 20 under collection of ~~samples~~ by the surface-tethered OSR, ~~the~~ great uncertainty of literature-based calibration factors, the few environments sampled, and the multitude of lighting and methodological factors affecting the relationship of attenuation and carbon, we needed to develop a particle sampling device which could operate on the CFE. The new integrated system is referred to as “CFE-Cal” (Fig. 1a).

Deleted: our

Deleted: sample

Deleted: a

Below we describe important design advances that led to the CFE-Cal and report first results from 2 CFE-Cals that were deployed and recovered 15 times at four locations during the June 2 to July 1 ~~2017~~ California Current Ecosystem Long Term Ecological Research (CCE-LTER) process study cruise aboard R/V *Revelle*. The aim of the CCE-LTER expedition was to characterize food web processes and particle export at different places within and outside of an offshore-flowing

Deleted: 2018

phytoplankton-rich filament of upwelled water near Point Conception, CA (Fig. 1b). The diverse environments sampled provided an excellent opportunity to collect a calibration sample dataset under high to low particle flux conditions.

2 Materials and Methods

2.1 CFE, CFE-Cal and Optical Attenuance

5 Bishop et al. (2016) describe in detail the CFE and the operation of its particle flux sensing OSR. These core elements are identical to those of the CFE-Cal. Briefly, once released from the ship the CFE dives repeatedly below the surface to obtain OSR observations at up to three target depths as it drifts with currents. The CFE's OSR awakes when the target depth is reached. Particles settle through a hexagonal celled baffle (1 cm opening) into a high-aspect ratio funnel (15.4 cm diameter opening) assembly before depositing on a 2.54 cm diameter glass sample stage. Particles are imaged at 13 μm pixel resolution
10 in three lighting modes: transmitted, transmitted-cross polarized, and dark field. ~~Here we focus on CFE-Cal results and on the calibration of volume attenuation (VA) determined from transmitted light imagery in terms of POC, PN, and PP sample loading. This study focuses on the calibration of VA: POC and PN. In future studies, cross polarized photon yield measured by the CFE, as discussed in Bishop et al. (2016) will be calibrated in terms of PIC units also using the sampler. As the samples collected on filters had large amounts of residual sea salt, the separation of the non-salt Ca requires very high accuracy and a separate protocol.~~
15

On first wake-up of a given CFE dive, the sample stage is flushed with water and images of the particle-free stage are obtained. At timed intervals (~25 min in data described here) the OSR repeats image sets, which register the sequential buildup of particles. ~~The 25-minute interval was determined to be consistent with previous CFE studies (Bishop et al., 2016).~~ After a
20 predetermined number of image sets over ~1.8 h, ~~stage~~ cleaning occurs and a new reference image set is obtained. After ~5-6 h at a target depth, the OSR performs a final image set, cleaning cycle and reference image set, and the CFE surfaces to report GPS position, CTD profile data and OSR engineering data, and dives to its next target depth. All target depths in this study were chosen to be at 150m. We describe in detail below the particle sampler and its integration with the CFE to form the CFE-Cal. In the case of the CFE-Cal, stage cleaning operations direct particles from each dive to a unique sample bottle.

25 Image attenuation was calculated following Bishop et al. (2016). Briefly, transmitted light images were normalized by a composite in-situ image of the particle free sample stage. The $-\log_{10}$ of the normalized image was taken to yield ~~attenuance~~ (ATN) values. Pixels with an ~~ATN~~ value less than 0.02 were defined to be background. Pixels with attenuation values above 0.02, determined to be particles, were integrated across the sample stage then divided by total number of pixels in the sample stage area yield ~~average~~ attenuation. This is multiplied by 1000 to yield ~~matN~~ and then by the sample stage area to give
30 sample Volume Attenuance (VA, units: ~~matN-cm²~~). ~~As light is reduced exponentially as it passes through particles, as long as the overlapping particles do not 100% obscure the transmitted light, attenuation affects are additive. In our analysis, the~~

Deleted: In this paper

Deleted: ,

Deleted: only

Deleted: vs

Deleted: volume attenuation determined from transmitted light imagery.

Deleted: the

Deleted: ATN

Deleted: light attenuation

Formatted: Font: Not Italic, Font color: Text 1

transmitted light even in the presence of multiple overlaid large aggregates, never went to zero (in other words, attenuation was never saturating). Therefore, overlapping particles are not an issue in this study.

Depth seeking performance of the CFE-Cal, imaging and sampling times and derived VA time series are illustrated in Figure A1. In order to compare VA to filter loads of POC, PN and PP, the cumulative VA over the course of a dive had to be calculated.

5 The tilt of CFE-Cals during drift is about 3°: the minimization of tilt is required to ensure optimal distribution of particles across the sample stage (Figure A2). During a dive, particles are transferred from image stage to a specific sample bottle between 2 to 6 times. For each cleaning cycle, the VA of a clean image was subtracted from the image with particles prior to transfer to a bottle. This then represented the amount of material directed into the sample bottle after cleaning. VA from each cleaning step was then summed to yield a cumulative VA which should correspond exactly to the particles directed into the
10 sample bottle (Table S1).

2.2 Sampler

Most key components of the sampler for the CFE-Cal were fabricated in the Advanced Prototyping Lab at the Jacobs Institute for Design Innovation at UC Berkeley using a Multi-Material Color Objet260 Connex3 (Stratasys, Israel); some parts were also fabricated using the Carbon model M1 3D printer (Redwood City, CA). We chose these particular additive manufacturing
15 processes because they were fast, low-cost, and enabled improved functional designs that were impossible to machine.

The new sampler incorporates the operation and water flow logic of a sampler built in 2004 for our surface buoy-tethered OSR but improves on it considerably (Fig. 7F in McDonnell et al. 2015; Bishop et al., 2016). The physical layout of the sampler is entirely new as the CFE-Cal had to meet stringent dimensional, buoyancy, compressibility, drag performance, and tilt criteria. Furthermore, as the sampler is intended to collect samples for particulate carbon, nitrogen, phosphorous, calcium carbonate,
20 silica, and trace metals, it needed to be non-contaminating.

Figure 2a shows detail of the integration of the sampler with 4 mounted sample collection bottles on the CFE-Cal; Figs. 2b and 2c detail the particle isolation system within each sample bottle. A planetary gear motor (2842S024C; Faulhaber Group, Micromo, Florida) and related custom electronics which actuate the sampler are housed in a pressure compensated acrylic tube filled with Fluorinert (3M) fluid and is mated coaxially with the rotor (Fig. 2d). Fluorinert was selected as it is clear (necessary
25 as there was an optical encoder in the pressure compensated chamber), low viscosity (for motor immersion) and inert (necessary as there were electronics in the chamber). The optical encoder provides feedback as to the proper location for the desired sampling bottle. Figure A3 shows details of the design of key 3D printed elements of the sampler. The sampler inlet is connected to the particle settling stage by a 40 cm long 9.5 mm inner diameter (ID) polyethylene tube (seen in Fig. 2a) and its

Formatted: Font: Not Italic, Font color: Text 1

Deleted: ,

Deleted:

Deleted: tilt performance,

Deleted: less than

Formatted: Font: Not Italic, Font color: Text 1

Deleted: 2

outlet is connected by a second 20 cm polyethylene tube to a SBE Model 5T (2000 RPM) pump (Sea Bird Electronics, WA). Flow rate during cleaning was $\sim 20 \text{ mL s}^{-1}$. When the CFE reaches depth on a new dive, the rotor is moved to select a water path that bypasses the sample bottles (Fig. A2, port 0) and the flow is directed to the outlet manifold. The bypass cleaning volume is $\sim 800 \text{ mL}$. After a cycle of particle accumulation and imaging, the motor driven sampler rotator opens to one of four sample bottle positions (1 – 4, Fig. A2) and the suction action of the pump draws water and particles from the imaging stage into the selected 250 mL conical clarified polypropylene centrifuge tube (Thermo Scientific, Nunc). A total of $\sim 400 \text{ mL}$ of water is drawn through the sampling system during each regular cleaning cycle and represents about a 30% of the volume of the collection funnel ($\sim 1460 \text{ cm}^3$). All particle transfers from a dive are directed to the same bottle (diamond points in Fig. A1). Particles are retained in the bottle by a 14 cm diameter circle of 51 μm polyester 33% open area mesh (SEFAR 07-51/33) wrapped and secured using silicone o-rings around the outlet structure within the bottle (Fig. 2c). The area of perforated outflow cylinder was $\sim 30 \text{ cm}^2$; however, when the circular mesh was secured to the top of the outlet cylinder by an o-ring, the pleated mesh area exposed to flow was $\sim 130 \text{ cm}^2$ (Fig. 2c).

The flow from imaging stage to bottle is constricted by the six 3 mm diameter openings that surround the sample stage. Loosely aggregated material is likely distorted or broken up into smaller pieces while being transferred. For cohesive particles (such as Siphonophores) and rigid particles (such as some Pteropod shells), the upper size limit is 3 mm. Though nothing was caught in the CFE-Cals during this study, there was one case where a larval crab was caught in one of the profiling CFEs and was not able to fit through the 3 mm diameter opening. This had to be removed after the CFE was retrieved.

2.3 Sampler Materials

Little is known about water absorption properties, dimensional stability, and chemical reactivity and contamination potential of the 3D printing resins as most are proprietary. The majority of sampler parts were fabricated using the Connex3 from FullCure 720 resin (Fig. A2) and some of the particle isolation assemblies were printed in both FullCure 720 and VeroWhite RGD35 resins. The Connex3 is a fused deposition modeling (FDM) printer which builds parts layer by layer. We fabricated three additional particle isolation assemblies from amber Cyanate Ester, black rigid Polyurethane and black Polylactic (PLA) resins on the Carbon printer; the process uses photopolymerization to form a solid piece as material is drawn from liquid resin. After parts were printed and support material removed, the parts were rinsed with deionized water and then leached in a 1.2 M HCl solution for 16 hours at room temperature. All remained stable to this treatment. Dimensional tests before and after sea trials showed that dimensions of the sampler body (Fig. A2) printed with FullCure 720 remained stable to within 0.06% of design dimensions.

Deleted: aggregates

Deleted:

Deleted: .

Deleted: tha

Deleted: t

2.4 Field Procedures

Prior to each deployment, the CFEs sample stage and related glass surfaces were cleaned to remove any remaining material collected during the previous deployment. Areas between glass layers were flooded with water to prevent air bubbles being trapped. Each CFE-Cal was outfitted with four clean sample collection tubes and filled with 0.4 µm filtered seawater. On recovery of the CFE-Cals, the sample bottles (Fig. 2d) were either immediately removed from the sampler and filtered or placed in a fridge at 10 °C to minimize sample degradation; in the latter case, samples were processed within 3 hours of collection.

All sample processing and manipulation took place in a laminar flow bench at sea. Each sample was decanted into an open filter funnel loaded with either 47 mm diameter Whatman Quartz Fiber (QMA, pore size ~1.2 µm) or Supor (pore size 0.4 µm) filters; transfer took place with filters under mild suction with the aim of evenly covering the filter surface (Fig. A3). Each sample tube and associated 51 µm mesh were further rinsed three times with ~ 5 mL of 0.4 µm filtered seawater to ensure quantitative transfer of particles. After filtration, the samples were quickly misted with ~3 mL of deionized water (DI) to reduce residual sea salt while still under suction. Samples were then placed in Gelman Petri slides and photographed wet under LED ring light illumination using a 20 Mpixel Sony RX100 V camera (pixel resolution of 19 µm), dried at 50 °C for 24 hours, and photographed again under the same lighting conditions in a laminar clean air bench. Dried samples were then stored in covered petri slides until analyzed in the laboratory. Prior to use, the QMA filters were placed in a muffle furnace at 450 °C overnight to reduce carbon blanks. Both the QMA (after combustion) and the Supor filters were leached in a 1.2 M HCl solution for 24 hours at room temperature and rinsed with deionized water and air dried in a class 100 laminar flow bench prior to use.

2.5 Laboratory Procedures

2.5.1 Carbon and Nitrogen Analysis

Briefly, half of each QMA filter was placed in a desiccator and exposed to HCl fumes (from 12 M HCl) for 24 hours to remove any carbonate carbon (Bishop et al. 1978) and then dried at 30°C for 36 hours and subsampled 6 to 8 times using a 3 mm diameter biopsy punch yielding ~1/16th of the whole sample. These were loaded into tin capsules and analyzed for total organic carbon and nitrogen using a Thermo Quest EA2500 Elemental Analyzer at Oregon State University according to Holser et al. (2011). A total of 27 unique cruise samples and process blanks (with 6 replicates), 5 unused QMA filters, and analytical blanks (empty tin capsules) were run. Process blanks were samples where no particles were directed to sample tube during deployment and processed as other samples. The other half of the sample was preserved for ICP-MS analysis.

Corrected POC was calculated following Eq (1):

$$POC_{corrected} = POC_{measured} - POC_{process\ blank}$$

Deleted: '

Deleted: t

Deleted: processed

Deleted: ¶

Moved down [3]: Samples ranged from 0.0267 to 0.1570 mmol C/filter (average ± sd: 0.0760 ± 0.0362) and 0.0029 to 0.0155 mmol N/filter (average ± sd: 0.0065 ± 0.0034). Process blanks contained 0.032 ± 0.008 mmol C/filter and 0.003 ± 0.0003 mmol N/filter. Unused QMA blanks were 0.0037 ± 0.0008 mmol C/filter and were below the detection limit for nitrogen; only 12% of carbon in the process blanks came from the blank filter. Nearly 90% of the process blank carbon is due either to accidental collection of particles during deployment, contamination during initial processing, or from DOC adsorption. Particles may enter a sample bottle while the sampler is turning and the selector briefly passes the blank bottle inlet. Data are tabulated in Table S1.¶

¶
Replicate analysis of 4 samples gave an average RSD of 0.14 and 0.07 for C and N, respectively which we assume is attributed to sample heterogeneity and can be applied to all samples. The RSD for replicate analyses of process blanks was 0.18 and 0.12 for C and N.¶

The sample POC error was calculated following Eq (2):

$$POC_{error} = \sqrt{(process\ blank\ s.d.)^2 + (sample\ RSD \times POC_{corrected})^2}$$

Nitrogen and phosphorous were calculated the same way, replacing POC with PN and PP.

5 2.5.2 ICP-MS Phosphorous Analysis

Samples on both Supor and QMA filters were analyzed using a Thermo Fisher Element II XR Inductively Coupled Plasma Mass Spectrometer (ICP-MS) at the UC Santa Cruz Marine Analytical Laboratory following Bishop et al. (2012). Half of each 47 mm filter was leached in 10 mL of a 0.6 M HCl solution at 60°C for 16 hours. The leach solution was then diluted with 18.2 mOhm-cm Milli-Q DI water to 50 grams; 1 mL of the diluted solution was then further diluted with 3 mL of 0.12 M HCl and spiked with 0.2 mL of 25 ppb In. Standards were prepared in the same acid matrix.

3 Results and Discussion

3.1 Samples Collected

Samples were collected from four productivity regimes and environmental conditions yielding a diverse array of particle sizes and classes (Fig. 3a-e). The flux rates between locations also varied widely. At location 1, flux was at times dominated by 1 mm diameter, 5-10 mm long anchovy pellets similar to those described by Saba and Steinberg (2012) with 95% of VA flux (average ~40 mATN-cm² cm² d⁻¹) being carried by particles > 1.5 mm in size. In contrast, at location 2, numerous small diameter (200-300 μm) olive green ovoid pellets dominated imagery and accounted for ~50% of the ~15 mATN-cm² cm² d⁻¹ VA flux. Location 3, in transitional waters near the filament edge, had a VA flux of ~2.3 mATN-cm² cm² d⁻¹ and ~65% of the flux carried by aggregates larger than 1.5 mm. At Location 4, in the most extended part of the filament, VA flux was ~22 mATN-cm² cm² d⁻¹, and 94% of the flux was carried by aggregates >1.5 mm in diameter.

The CFE-Cals were new and there were initial malfunctions (i.e. instrument not diving to depth, not stabilizing at depth, or sampler not switching target bottles correctly) which were mostly resolved during the first half of the expedition. In all, The CFE-Cals were deployed 15 times over the course of the June 2017 CCE-LTER study, the CFE was outfitted with 4 sample bottles for each deployment. For each deployment, depending on how much time was available, the CFE-Cals performed 3 to 4 dives. Of these 60 possible sample collections, 10 were not useable due to a CFE-Cal malfunction, and one was not useable due to a swimming organism. Almost all these malfunctions occurred at the beginning of the cruise. Table 1 details all these points as well as noting sampling times, depths and filter type. The CFE-Cal instruments were built using the new SOLO2 floats whereas the original CFEs were built using SOLO1 floats. We found that the concave bladder housing of the new SOLO2 float design trapped air and made it more difficult for the CFE to attain its target depth. Once we realized this issue, before each deployment, the bottom of the float was flushed with water prior to each deployment and care was made to launch the

Moved down [2]: Phosphorous in samples ranged 40-fold from 3.9×10^{-9} to 1.5×10^{-7} (average \pm sd: $2.0 \times 10^{-8} \pm 2.4 \times 10^{-8}$). Unlike C and N, the process blanks were location specific with averages of 8.9×10^{-8} , 5.0×10^{-8} , 1.9×10^{-8} and 5.0×10^{-8} mmol P/filter for location 1, 2, 3 and 4 respectively.

Deleted: ¶

Moved (insertion) [4]

Deleted: The CFE-Cals were new and there were instances of The CFE-CALS were deployed 15 times over the course of the June 2017 CCE-LTER study, CFE-Cal malfunction (i.e. instrument not diving to depth, not stabilizing at depth, or sampler not switching target bottles correctly) which were resolved during the expedition, or swimmers such as a large siphonophores (see Table 1 for details) led to severalome dives not yielding usable samples.

Deleted: AL

float horizontally to prevent this. As all instrument malfunctions were identified and resolved, future deployments will be far more robust.

A total of 15 QMA samples were analysed for POC and PN. These 15 QMA samples and 19 Supor samples were analysed for PP. Samples ranged from 0.0267 to 0.1570 mmol C/filter (average \pm sd: 0.0760 \pm 0.0362) and 0.0029 to 0.0155 mmol N/filter (average \pm sd: 0.0065 \pm 0.0034). Phosphorous in samples ranged 40-fold from 3.9×10^{-5} to 1.5×10^{-3} mmol P/filter (average \pm sd: $2.0 \times 10^{-4} \pm 2.4 \times 10^{-4}$). Results are shown in table S1.

Process blanks were subtracted from the sample values as shown in equation 1. As there were only 5 QMA process blanks, an average of the five was used to blank correct POC and PN. This drove one POC and one PN sample from Location 3 negative, though not negative within error. Fluxes at location 3 were very low - an order of magnitude lower than samples collected in other regions. Process blanks contained 0.032 ± 0.008 mmol C/filter and 0.003 ± 0.0003 mmol N/filter. Unused QMA blanks were 0.0037 ± 0.0008 mmol C/filter and were below the detection limit for nitrogen; only 12% of carbon in the process blanks came from the blank filter. Nearly 90% of the process blank carbon is therefore not from the blank filter, but stems from either accidental collection of particles during deployment or contamination during processing. Particles may be accidentally collected by entering a sample bottle while the sampler is turning and the selector briefly passes the blank bottle inlet. As there were at least two process blanks per location for PP, blanks could be location specific. The process blanks were 8.9×10^{-5} , 5.0×10^{-5} , 1.9×10^{-5} and 5.0×10^{-5} mmol P/filter for location 1, 2, 3 and 4 respectively.

Replicate analysis of 4 samples gave an average RSD of 0.14 and 0.07 for C and N respectively. Punched subsamples are collected evenly distributed across the filter, but inevitably as there are discrete particles on the filter, there is some heterogeneity between the sub-samples (Figure A5). The RSD of replicate analysis we assume is attributed to this sample heterogeneity and can be applied to all samples. The RSD for replicate analyses of process blanks was 0.18 and 0.12 for C and N respectively.

3.2 Transfer Efficiency

To validate the efficiency of transfer of particles imaged to sample bottles, ovoid pellets were manually counted (Fig. 4) in both the CFE's OSR images and of photographs of filters of material sampled at location 2. CFE-Cal2 collected close to the same number of particles in the sampler as were imaged (on average, there was less than a 9% difference between particles imaged and particles filtered, particles were not exclusively higher in one or the other). CFE-Cal4, however, collected 1.45 times more ovoid pellets in the sampler than were imaged. The sampler uses an optical encoder to sense a home position from which it advances to select specific bottles. Software is programmed with a time out in the case that the "home" position cannot be found to prevent continuous operation and depletion of the CFE batteries. During pre-cruise tests of the CFE-Cal no

Deleted: ¶

In one dive, mentioned above, a gelatinous swimming siphonophore entered the imaging stage and remained throughout the dive, rendering the sample not useable.

Deleted: Altogether, there were 19 valid QMA samples (15 samples, 4 blanks) and 27 Supor samples (19 samples, 8 blanks).

Deleted: There was a

Deleted: which

Deleted: .

Deleted: PP was analysed for the

Deleted: as the

Moved (insertion) [3]

Deleted: This one sample that was driven negative was collected from location 3.

Deleted: Process blanks contained 0.032 ± 0.008 mmol C/filter and 0.003 ± 0.0003 mmol N/filter. Unused QMA blanks were 0.0037 ± 0.0008 mmol C/filter and were below the detection limit for nitrogen; only 12% of carbon in the process blanks came from the blank filter. Nearly 90% of the process blank carbon is due either to accidental collection of particles during deployment, contamination during initial processing, or from DOC adsorption. Particles may enter a sample bottle while the sampler is turning and the selector briefly passes the blank bottle inlet. Data are tabulated in Table S1.

Formatted: Font: Not Italic, Font color: Text 1

Formatted: Font: Not Italic, Font color: Text 1

Deleted: , respectively

Deleted: which

Deleted: ¶

Deleted: ¶

Moved (insertion) [2]

Deleted: Phosphorous in samples ranged 40-fold from 3.9×10^{-5} to 1.5×10^{-3} (average \pm sd: $2.0 \times 10^{-4} \pm 2.4 \times 10^{-4}$). Unlike C and N, the process blanks were location specific with averages of 8.9×10^{-5} , 5.0×10^{-5} , 1.9×10^{-5} and 5.0×10^{-5} mmol P/filter for location 1, 2, 3 and 4 respectively.

Moved up [4]: The CFE-CALs were deployed 15 times over the course of the June 2017 CCE-LTER study, CFE-Cal malfunction (i.e. instrument not diving to depth, not stabilizing at depth, or sampler not switching target bottles correctly) or swimmers such as

Deleted: Collection

Deleted:

Deleted: 00

Deleted: 00

Deleted: in

Deleted: We don't fully understand this but known sampler ... [1]

Deleted: cfeS

positioning errors were registered. However, these tests were done in a lab, with room temperature fresh water and not in 10°C seawater under pressure. It is clear that the sampler for CFE Cal4 stopped short of home position, and this likely led to the over transfer of particles that were not imaged. We recognized this issue during deployment operations at cycle 3 and after the time-out limit was adjusted; this problem was not encountered again. The known sampler positioning issues at this time may have led to transfer of pellets to bottles from times (such as during float ascent to the surface) when particles were not imaged by CFE-Cal4. To correct for this, the POC, PN and PP numbers for CFE-Cal4 at location 1, 2 and 3 were divided by 1.45.

Bishop et al., (2012) investigated the effect of filtration rate on aggregate retention during large volume in-situ filtration sampling and found that aggregates were broken up when the flow velocity through 51 µm mesh exceeded 1 cm s⁻¹ over a four-hour sampling time. During CFE-Cal stage cleaning, the sample transfer pump is operated for two cycles of ten seconds at a flow rate of ~20 mL s⁻¹. The mesh area on the outflow from the sample bottle is approximately 130 cm². We thus calculate the flow speed through the mesh to be ~0.15 cm sec⁻¹, 15% of the threshold speed recommendation by Bishop et al. (2012). Although intact large aggregates were not seen on the sample filters (compare Fig. A3d vs. Fig. 3d), given our limited sample transfer time (< 2 minutes) and low flow velocity, we believe that our transfer efficiency for the particles comprising the loosely aggregated material is similar to that for the more robust pellets.

3.3 Calibration Results

Figure 5 shows cumulative VA regressed against sample POC, PN and PP (data in Table S1). All of our results are forced through zero as both VA and elemental values are blank controlled. Regressions results yielded slopes and R² values and number of samples (in parentheses) of 1.01 x 10⁴ mATN-cm²: mmol POC (r²=0.86, n=12, p<0.001) and 1.01 x 10⁵ mATN-cm²: mmol PN (r²=0.86, n=15, p<0.001). Three of 15 samples had C/N ratios above 20 and were not used in the regression for POC as these numbers are not typical of sinking particles (e.g. Bishop et al., 1977, Lamborg et al., 2008, Stukel et al., 2013). Stukel et al. (2013) reported trap POC/PN mole ratios ranging from 5-14 (average, 9.6) at 100 m in the same upwelling regime we have sampled; Lamborg et al. (2008) reported POC/PN ratios ranging from 7.7 to 8.5 in productive waters of the Oyashio and Oligotrophic waters of the North Pacific Gyre. The molar ratio of C/N from our regression slopes is 9.9, in line with Stukel et al. (2013).

The high C/N values of excluded samples may have been due to contamination by residual material used as a scaffold to build the 3D printed parts: in one case, a 1 mm sized aggregate of such material was found on our filters. New lighting systems were rapidly prototyped just prior to cruise. The scaffold material, Stratasys' OBJET Support SUP706 is made of 1,2-Propylene glycol and Polyethylene glycol, Methanone, (1-hydroxycyclohexyl) phenyl-both of which contain carbon but not nitrogen (SUP706 SDS <https://store.stratasys.com/medias>). The material also contains an unspecified acrylic. As the 3D printed material contains no nitrogen, C/N values would be elevated if they were contaminated. Including the three high C/N

Deleted: S

Deleted: which

Formatted: Font: Not Italic, Font color: Text 1

Deleted: by increa

Deleted: sing

Deleted: adjusted

Formatted: Font: Not Italic, Font color: Text 1

Formatted: Font: Not Italic, Font color: Text 1

Deleted: A software problem was identified and addressed prior to location 4 deployments and no correction was applied.

Deleted: collection

Formatted: Font color: Text 1, Superscript

Deleted: .066

Formatted: Font color: Text 1, Superscript

Deleted: 0

Deleted: .5

Formatted: Font color: Text 1, Superscript

Deleted: 00

Formatted: Font color: Text 1, Superscript

Deleted: 7

Deleted: 6

Deleted: (2008)

Deleted: 2

Deleted: ,

Deleted: ,

Formatted: Font: Not Italic, Font color: Text 1

Formatted: Font: Not Italic, Font color: Text 1

Deleted: The C/N of the other 12 samples were all consistent with natural populations. These are in line with C/N that have been found in the region previously (Stukel et al., 2013).

ratio points in the VA:POC regression reduces the slope to 0.86×10^4 with an R^2 of 0.64 ($n=15$, $p<0.001$), we report this even though we do not believe this to be representative of natural particulates.

The data also demonstrate that there is no obvious difference for VA:PN or VA: POC for samples collected from Locations 1 and 4 (Fig. 1, Fig. 4) where aggregates > 1.5 mm in size accounted for 95% of the flux compared to Locations 2 and 3 where smaller material contributed 50 and 30% of the flux, respectively.

The relationship for VA: PP was scattered with a slope of 1.53×10^6 mATN-cm²: mmol PP ($R^2=-0.07$, negative R^2 values denote results worse than horizontal fit). The sample with anchovy fecal pellets had a POC/PP ratio of 90 mol/mol, far higher than all other samples (~300 mol/mol). The fact that PP had zero correlation with VA is consistent with the strong loss of P relative to carbon and nitrogen as large aggregates sink (e.g. Bishop, 1977; Lam et al., 2007). Scanning electron microscopy showed that the anchovy fecal pellets were stuffed with diatoms and as they are larger and sink at a much faster rate (up to 500m d⁻¹), it follows that this sample should have a higher PP content as there is less time for microbial degradation and remineralization, and when this point is arbitrarily removed, the relationship of VA: PP for non-Anchovy aggregates improved 3.23×10^6 mATN-cm²: mmol PP ($R^2=0.41$). Though the ultimate goal is to allow an estimation of biogeochemical fluxes based on image analysis, because of the known lability of PP relative to POC or PN in sinking particles, we conclude that PP cannot be predicted from VA.

As mentioned earlier, we found that CFE-Cal4 collected 1.45 times more ovoid pellets on the filters than were imaged due to a sampling issue and that we therefore divided the CFE-Cal4 POC and PN samples for location 1, 2 and 3 by this empirically derived factor. This affected 6 samples in the POC and PN regressions (see table S1). We note that if instead of applying this empirical factor, these samples are removed from the regression, the VA: POC and VA:PN slopes both change less than 5%. The slopes (number of samples and R^2 in parenthesis) change to 1.06×10^4 ($n=8$, $R^2=0.93$) and 1.04×10^5 ($n=9$, $R^2=0.91$). Using these data which have been corrected using the empirical factor therefore affects the overall regression very little.

3.4 Comparison to previous studies

Two autonomous flux monitoring systems, the CFE (Bishop et al., 2016) and the OST (Estapa et al., 2017), have now been calibrated to relate the attenuation flux to the flux of particulate organic carbon. This study expands upon Estapa et al. (2017) as samples from a wide range of environments and with a far greater range of aggregate size distributions have been collected. The highest POC flux collected in Estapa et al.'s (2017) calibration was under 2 mmol C m⁻² d⁻¹. The flux environments sampled in our study ranged from <2 to 40 mmol C m⁻² d⁻¹.

Deleted: s...in the VA:POC regression changes...educes the slope to 0.8,...55 ... [2]

Deleted: 2...with an R^2 of 0.64 ($n=15$, $p<0.001$) ... [3]

Formatted: Font color: Text 1, Superscript

Formatted: Left, Space Before: 6 pt, After: 6 pt

Deleted: ¶

The high C/N values of excluded samples may have been due to contamination by residual material used as a scaffold to build the 3D printed parts; in one case, a 1 mm sized aggregate of such material was found on our filters. The scaffold material, Stratasys' OBJET Support SUP706 is made of 1,2-Propylene glycol and Polyethylene glycol.

Formatted: Font color: Text 1, English (US)

Deleted: 1.54×10^6 ,000

Formatted: Font color: Text 1, Superscript

Deleted: r

Deleted: in one

Formatted: Font color: Text 1, Superscript

Deleted: ay..., it follows that this sample should have a higher PP

Deleted: ,

Formatted: Font color: Text 1, Superscript

Deleted: ,000

Deleted: r

Formatted: Font color: Text 1, Superscript

Moved (insertion) [10]

Deleted: The fact that PP had the lowest correlation with VA is [6]

Deleted: ; Hannah keep the original figure;

Formatted: Font color: Text 1, Highlight

Deleted: Even when eliminating that particular point, the ... [7]

Formatted: Font: Not Italic, Font color: Text 1

Deleted: highly

Formatted: Font: Not Italic, Font color: Text 1

Deleted: heterogeneous nature

Formatted: Font: Not Italic, Font color: Text 1

Deleted: phosphorous

Formatted: ... [8]

Deleted: such as the anchovy pellet,

Formatted: ... [9]

Moved up [10]: The fact that PP had the lowest correlation with

Deleted: ¶ ... [10]

Deleted: r...range of environments have been collected ...nd ¶ [11]

Deleted: ¶

Figure 6 compares the relationship between VA flux and carbon flux from this study (data for regression in Table S1) vs. data from Estapa et al. (2017). When converted to compatible units, the slope for Estapa's VA flux (mATN-cm² cm² d⁻¹) versus POC flux (mmol C m⁻² d⁻¹) is 1.50 (allowing for an intercept) and 2.19 (forced through zero) and, while our slope is 1.03 (forced through zero), Estapa et al. (2017) calculates attenuation by taking the natural log of transmittance and observations are reported in units of ATN m² m⁻² d⁻¹. Our data are the log₁₀ of transmittance as documented in Bishop et al. 2016 and reported in units of mATN cm² cm⁻² d⁻¹. Therefore, Estapa's published data has been divided by 2.303 to convert the natural log attenuation to log₁₀ attenuation and multiplied by 1000 to scale to mATN units. The dimensional data do not require scaling. Our observations were for depths near 150 meters and it is unknown if there is a depth dependence to calibration factors. We note that Estapa et al. (2017) combined samples from ~150, 300 and 500 meters in her regression. This said, the slopes of our two datasets differ by a factor of 1.5 to 2. In our data, attenuation of particles in the red image plane is 6% lower than in green, thus wavelength of analysis is a minor factor explaining the differences. Given the large range in particle size distributions and classes (e.g. samples dominated by dense Anchovy pellets vs. 2-3 mm size amorphous semi-transparent aggregates), we can rule out particle size effects. Beam geometry and the other factors underlying our different methodologies likely explain the differences found.

As noted earlier, Bishop et al. (2016) estimated the factor for conversion of POC flux (C mmol m⁻² d⁻¹) to VA flux (mATN-cm² cm² d⁻¹) using two previously published values of carbon: particle volume as there were not calibration samples available. The two methods are described briefly. In method one, Bishop et al. (2016) calculated an aggregate volume of 0.113 cm³ for particles >800 μm (which accounted for 97% of VA) in a series of 5 images. An aggregate density of 0.087 g cm⁻³ and 60% organic matter of dry weight was assumed based on Bishop et al., (1978). To convert the organic matter weight to carbon, a conversion factor of 1.88 was used from Hedges et al. (2002). Using these values yielded an estimated flux of 183 mmol C m⁻² d⁻¹, compared to a VA flux of 66.2 mATN-cm² cm² d⁻¹, which gives a POC flux (C mmol m⁻² d⁻¹) to VA flux (mATN-cm² cm² d⁻¹) of 2.8 (183: 66.2 × 0.97 = 2.8). For comparison, POC was also estimated following the methods of Alldredge (1998). Alldredge (1998) derived a regression formula relating the equivalent spherical volume (ESV) and POC content of particles:

$$POC_{\mu g} = 0.99 \times ESV^{0.52}$$

The Alldredge (1998) relationship has previously been used to estimate carbon content from aggregates in gel trap imagery (Ebersbach and Trull, 2008; Ebersbach et al., 2011) and aggregates collected then imaged using Marine Snow Catchers (Riley et al., 2012; Baker et al., 2017). In the Bishop et al. (2016) study, the POC density of aggregates was 0.028 g C cm⁻³ following method 1, and 0.0002 g C cm⁻³ using the Alldredge (1998) formula. The two order of magnitude difference was likely due to the fact that the relationship between aggregate volume to POC for Alldredge (1998) was based on aggregates collected between 10 and 20 m, photographed in-situ in a plane parallel to their sinking direction, whereas the Bishop et al. (2016) method was based on published values of large particles collected using large volume filtration between 100 and 400 m depth. The conversion factor for POC:VAF for Alldredge was 17 times lower than the Bishop et al. 2016 factor of 2.8 (Bishop et al.,

Deleted: 1.50 (allowing for an intercept)

Deleted:

Deleted: mATN

Deleted: e,

Deleted: transforms

Formatted: Font: Not Italic, Font color: Text 1

Deleted: only

Deleted: ¶

Deleted: to be 2.8;

Deleted: Below,

Deleted: t

Deleted: ¶

Deleted: , Baker et al., 2017

Formatted: Font color: Text 1, Superscript

2016). Analysis of directly imaged and sampled material in this study yielded a slope of 1.03 for VAF:POC, which is about 3 times higher than estimated using Bishop et al., (1978) but 6 times lower than inferred from Allredge et al. (1998) (Figure 6). It is not surprising our results are not consistent with Allredge (1998) as our samples were collected more than 100m deeper and Allredge's volumes were calculated based on images taken in-situ parallel to the aggregate sinking direction whereas the CFE images are collected looking upwards after the aggregates have settled onto the glass stage. Though the settling motion is gentle and does not break apart the aggregate, there is very likely some compaction as the particle settles onto the stage.

Deleted: the reverse conversion factor is 0.357 consistent with slopes depicted in figure 6.

Deleted: 's

Deleted:

Deleted: relationship for marine snow sampled by scuba from shallow depths. Our results are not consistent with the published Allredge (1998) relationship.

Bishop et al. (2016) reported CFE attenuation fluxes averaging $66.2 \text{ mATN-cm}^2 \text{ cm}^{-2} \text{ d}^{-1}$ at 150 m in the Santa Cruz Basin in January 2013 and estimated a POC flux of $190 \text{ mmol C m}^{-2} \text{ d}^{-1}$, about 8 times higher than the highest previously measured flux from surface-tethered sediment traps deployed over a 3-year period at 100 and 200 meters in nearby waters (Thunell, 1998; August 1993 to September 1996). Converting the $66.2 \text{ mATN-cm}^2 \text{ cm}^{-2} \text{ d}^{-1}$ attenuation flux to POC flux using our new calibration yields $64.3 \text{ mmol C m}^{-2} \text{ d}^{-1}$, a value which is still three times higher than the highest previously measured flux (Thunell, 1998). In short, the likely discrimination of surface tethered baffled sediment traps against the collection of $>1 \text{ mm}$ sized particles remains an issue in biologically dynamic regimes dominated by large aggregates.

Deleted: 68.219

4 Conclusions and future development

We have presented the initial calibration of the CFE optical proxy for particulate carbon and nitrogen using the newly developed CFE-Cal instruments. The development of a sampling system for the Carbon Flux Explorer has overcome a major barrier to the calibration of our attenuation proxy for organic matter export. The calibration of volume attenuation flux (VAF) against organic carbon and nitrogen flux in this study represents an important step forward in the development of autonomous optical flux measurements. Our regression results yield well-correlated calibrations for POC and PN ($\text{POC } R^2 = 0.86, n=12, p<0.001$ and $\text{PN } R^2 = 0.86, n=15, p<0.001$) that apply over a wide range of environments, including high flux environments in recently upwelled water as well as low flux off-shore transitional waters. Phosphorus was shown to be poorly correlated, consistent with the highly labile nature of this element relative to either C or N. Our results give us confidence that images collected by the CFE can be used to calculate the fluxes of carbon and nitrogen. We find less than a two-fold difference in the POC flux vs. Volume Attenuance flux regression slope from Estapa et al. (2017). This is remarkable given the strongly different environments, methodology, and means by which fluxes were sampled. Both these studies reinforce the theory that light attenuation can be used as a proxy for POC and in our case PN flux.

Deleted: , nitrogen and phosphorus

Deleted: strong

Deleted: 7

Deleted: a .

Deleted: If TEP does contribute to POC flux in our samples, then our results suggest that attenuation is a better proxy for particulate nitrogen flux.

Deleted: In addition, our calibration is shown to be insensitive to particle size distribution and particle classes dominating export.

Optimization of CFE-Cal sample return, performance validation, and simplification of recovery logistics during CCE-LTER required that all samples in this dataset to be collected near 150 m. These calibration samples were all collected off the coast

of California, during the month of June near 150 meters. To make the calibration more robust and determine whether the calibration relationships derived here are widely applicable, it is essential to extend these results to greater depths, and to different oceanic regions, environments and ecosystem structures. Intercalibration of the CFE attenuation measurements with other autonomous systems should be pursued.

Results presented above demonstrate that the magnitude of flux and of food web processes responsible for flux can vary strongly over relatively small spatial and temporal scales in dynamic coastal waters. Thus, the use of high frequency autonomous observations will significantly better inform food web and carbon export simulations. Our promising initial calibration of VAF in terms of POC and PN justifies further development of instruments which optically measure POC such as the Carbon Flux Explorer.

Acknowledgements

We would like to thank Mark Ohman (chief scientist), members of the science party, and captain and crew of the R/V Revelle for facilitating CFE-Cal deployments during the June 2 – July 1 2017 California Current Ecosystem Long Term Ecological Research process study. Lee-Huang Chen (UC Berkeley, Engineering) contributed at critical stages of this project. We thank Alejandro Morales (LBNL), Christopher Parsell and the Jacobs Institute for Design Innovation (UC Berkeley), Christopher Myers (UC Berkeley), Mike McLune (SIO), Phoebe Lam and Rob Franks (UC Santa Cruz). We'd also like to thank the many UC Berkeley undergraduates who have worked with us at sea and in the laboratory, in particular, Casey Fritz, Beth Connors, Xiao Fu, Sylvia Targ, Jessica Kendall-Bar, and William Kumler. US National Science Foundation grant OCE 0936143 supported Carbon Flux Explorer development; OCE 1528696 supported the development and at sea work with the CFE-Cal systems. The CCE-LTER is supported by US NSF grant OCE 16-37632.

References

Allredge, A.L., Passow, U. and Logan, B.E.: The abundance and significance of a class of large, transparent organic particles in the ocean, Deep Sea Res. Part I Oceanogr. Res. Pap., 40(6), 1131-1140, doi:10.1016/0967-0637(93)90129-Q, 1993.

Allredge, A.L.: The carbon, nitrogen and mass content of marine snow as a function of aggregate size, Deep Sea Res. Part I Oceanogr. Res. Pap., 45(4-5), 529-541, doi:10.1016/S0967-0637(97)00048-4, 1998.

[Baker, C. A., Henson, S. A., Cavan, E. L., Giering, S. L. C., Yool, A., Gehlen M., Belcher, A., Riley, J. S., Smith, H. E. K., and Sanders, R.: Slow-sinking particulate organic carbon in the Atlantic Ocean: Magnitude, flux, and potential controls, Global Biogeochem. Cycles, 31, 1051–1065, doi:10.1002/2017GB005638, 2017.](#)

Deleted: As all calibration samples in this dataset were made at 150 m Results presented above demonstrate that the magnitude of flux and of food web processes responsible for flux can vary strongly over relatively small spatial and temporal scales in dynamic coastal waters., in the future we plan calibration studies to include more depths to 1000 meters.

Moved (insertion) [1]

Moved up [1]: Results presented above demonstrate that the magnitude of flux and of food web processes responsible for flux can vary strongly over relatively small spatial and temporal scales in dynamic coastal waters.

Deleted: successful

Deleted: expanded

Deleted: deployments

Deleted: in remote and stormy seas

Deleted: at UC Berkeley

- Banse, K.: Reflections About Chance in My Career, and on the Top-Down Regulated World, *Ann. Rev. Mar. Sci.*, 5(1), 1–19, doi:10.1146/annurev-marine-121211-172359, 2013.
- Bishop, J.K.B., Edmond, J.M., Ketten, D.R., Bacon, M.P. and Silker, W.B.: The chemistry biology and vertical flux of particulate matter from the upper 400m of the equatorial Atlantic Ocean, *Deep Sea Res.*, 24, 511–548, 1977.
- Bishop, J.K.B., Stepien, J.C. and Wiebe, P.H.: Particulate matter distributions, chemistry and flux in the panama basin: response to environmental forcing, *Progress in Ocean.*, 17(1-2), 1-59, doi:10.1016/0079-6611(86)90024-8, 1986.
- Bishop J.K.B, J., E. Calvert S., S. and Soon, M. Y. S.: Spatial and temporal variability of POC in the northeast subarctic Pacific, *Deep. Res. Part II Top. Stud. Oceanogr.*, 46(11–12), 2699–2733, doi:10.1016/S0967-0645(99)00081-8, 1999.
- 10 Bishop, J.K.B. and Wood, T. J.: Particulate matter chemistry and dynamics in the twilight zone at VERTIGO ALOHA and K2 sites, *Deep. Res. Part I Oceanogr. Res. Pap.*, 55(12), 1684–1706, doi:10.1016/j.dsr.2008.07.012, 2008.
- Bishop, J.K.B. and Wood, T. J.: Year-round observations of carbon biomass and flux variability in the Southern Ocean, *Global Biogeochem. Cycles*, 23(2), 1–12, doi:10.1029/2008GB003206, 2009.
- Bishop, J. K.B., Ketten, D. R. and Edmond, J. M.: The chemistry, biology and vertical flux of particulate matter from the upper 400 m of the Cape Basin in the southeast Atlantic Ocean, *Deep. Res.*, 25(12), doi:10.1016/0146-6291(78)90010-3, 1978.
- 15 Bishop, J. K. B., Davis, R. E. and Sherman, J. T.: Robotic observations of dust storm enhancement of carbon biomass in the North Pacific., *Science*, 298(5594), 817–821, doi:10.1126/science.1074961, 2002.
- Bishop, J. K. B., Wood, T. J., Davis, R. E. and Sherman, J. T.: Robotic observations of enhanced carbon biomass and export at 55 degrees during SOFeX., *Science*, 304(5669), 417–420, doi:10.1126/science.1087717, 2004.
- 20 Bishop, J. K. B., Lam, P. J. and Wood, T. J.: Getting good particles: Accurate sampling of particles by large volume in-situ filtration, *Limnol. Oceanogr. Methods*, 10, 681–710, doi:10.4319/lom.2012.10.681, 2012.
- Bishop, J. K. B., Fong, M. B. and Wood, T. J.: Robotic observations of high wintertime carbon export in California coastal waters, *Biogeosciences*, 13(10), 3109–3129, doi:10.5194/bg-13-3109-2016, 2016.
- Boss, E., Guidi, L., Richardson, M. J., Stemann, L., Gardner, W., Bishop, J. K. B., Anderson, R. F. and Sherrell, R. M.: Optical techniques for remote and in-situ characterization of particles pertinent to GEOTRACES, *Prog. Oceanogr.*, 133, 43–54, doi:10.1016/j.pocean.2014.09.007, 2015.
- Briggs, N., Perry, M. J., Cetinić, I., Lee, C., D’Asaro, E., Gray, A. M. and Rehm, E.: High-resolution observations of aggregate flux during a sub-polar North Atlantic spring bloom, *Deep Sea Res. Part I Oceanogr. Res. Pap.*, 58(10), 1031–1039, doi:https://doi.org/10.1016/j.dsr.2011.07.007, 2011.
- 30 ~~Buessler, K.O., Antia, A. N., Chen, M., Fowler, S. W., Gardner, W. D., Gustafsson, O., Harada, K., Michaels, A. F., Rutgers van der Loeff, M., Sarin, M., Steinberg, D. K. and Trull, T.: An assessment of the use of sediment traps for estimating upper ocean particle fluxes, *J. Mar. Res.*, 65(3), 345–416, doi:10.1357/002224007781567621, 2007.~~
- Burd, A. B., Hansell, D. A., Steinberg, D. K., Anderson, T. R., Aristegui, J., Baltar, F., Beaufré, S. R., Buesseler, K. O., DeHairs, F., Jackson, G. A., Kadko, D. C., Koppelman, R., Lampitt, R. S., Nagata, T., Reinthaler, T., Robinson, C., Robison, B. H., Tamburini, C. and Tanaka, T.: Assessing the apparent imbalance between geochemical and biochemical indicators of
- 35

Deleted: Buesseler, K. O.,

meso- and bathypelagic biological activity: What the @S#! is wrong with present calculations of carbon budgets?, Deep Sea Res. Part II Top. Stud. Oceanogr., 57(16), 1557–1571, doi:https://doi.org/10.1016/j.dsr2.2010.02.022, 2010.

Ebersbach, F., Trull, T. W., Davies, D. M. and Bray, S. G.: Controls on mesopelagic particle fluxes in the Sub-Antarctic and Polar Frontal Zones in the Southern Ocean south of Australia in summer-Perspectives from free-drifting sediment traps, Deep. Res. Part II Top. Stud. Oceanogr., 58(21–22), 2260–2276, doi:10.1016/j.dsr2.2011.05.025, 2011.

[Ebersbach, F. and Trull, T.W.: Sinking particle properties from polyacrylamide gels during the DERguelen Ocean and Plateau compared Study \(KEOPS\): Zooplankton control of carbon export in an area of persistent natural iron inputs in the Southern Ocean, Limnol. Oceanogr., 53\(1\), 212-224, doi: 10.4319/lo.2008.53.1.0212, 2008.](#)

Estapa, M., Durkin, C., Buesseler, K., Johnson, R. and Feen, M.: Carbon flux from bio-optical profiling floats: Calibrating transmissometers for use as optical sediment traps, Deep. Res. Part I Oceanogr. Res. Pap., 120(December 2016), 100–111, doi:10.1016/j.dsr.2016.12.003, 2017.

Estapa, M. L., Buesseler, K., Boss, E. and Gerbi, G.: Autonomous, high-resolution observations of particle flux in the oligotrophic ocean, Biogeosciences, 10(8), 5517–5531, doi:10.5194/bg-10-5517-2013, 2013.

Dunne J.P., Armstrong, R.A., Gnanadesikan, A. and Sarmiento J.L.: Empirical and mechanistic models for the particle export ratio, Global Biogeochem. Cycles, 19(4), doi:10.1029/2004GB002390, 2005.

Falkowski, P. G., Barber, R. T. and Smetacek, V.: Biogeochemical Controls and Feedbacks on Ocean Primary Production, Science, 281(5374), 200-206, doi: 10.1126/science.281.5374.200, 1998.

Gardner, W. D., Richardson, M. J. and Smith, [W. O. Jr.](#): Seasonal patterns of water column particulate organic carbon and fluxes in the Ross Sea, Antarctica, Deep. Res. Part II Top. Stud. Oceanogr., 47(15–16), 3423–3449 [online] Available from: <http://www.sciencedirect.com/science/article/B6VGC-41WBFCW-J/2/24062ec421c6faf7d4e3f12a28f09509>, 2000.

Holser, R. R., Goni, M. A. and Hales, B.: Design and application of a semi-automated filtration system to study the distribution of particulate organic carbon in the water column of a coastal upwelling system, Mar. Chem., 123(1–4), 67–77, doi:10.1016/j.marchem.2010.10.001, 2011.

Lam, P.J and Bishop, J.K.B.: High biomass, low export regimes in the Southern Ocean, Deep Sea Res. Part II, 54, 601-638, doi: 10.1016/j.dsr2.2007.01.013, 2007.

[Lamborg, C.H., Buesseler, K.O., Valdes, J., Bertrand, C.H., Manganini, S., Pike, S., Bidigare, R., Steinberg, D., Wilson, S., Trull, T.: The flux of bio- and lithogenic material associated with sinking particles in the mesopelagic “twilight zone” of the northwest and North Central Pacific Ocean, Deep Sea Res. Part II, 55\(4\), 1540-1563, doi:10.1016/j.dsr2.2008.04.011, 2008](#)

Mcdonnell, A. M. P., Boyd, P. W. and Buesseler, K. O.: Effects of sinking velocities and microbial respiration rates on the attenuation of particulate carbon fluxes, Global Biogeochemical Cycles, 29(2), 175–193, doi:10.1002/2014GB004935, 2015.

Passow, U. and Carlson, C.A.: The biological pump in a high CO₂ world, Mar. Ecol. Prog. Ser., 470, 249–271, doi: 10.3354/meps00985, 2012.

[Riley, J. S., Sanders, R., Marsay, C., Le Moigne, F. A. C., Acherberg, E. P., and Poulton, A. J.: The relative contribution of fast and slow sinking particles to ocean carbon export, Global Biogeochem. Cycles, 26, GB1026, doi:10.1029/2011GB004085, 2012.](#)

- Deleted:
- Deleted: Walker
- Deleted: . J.
- Deleted: Lamborg, H. C.,
- Moved down [5]: K. O.
- Moved down [6]: C. H.
- Moved (insertion) [5]
- Moved (insertion) [6]
- Deleted: J.
- Deleted: S.
- Deleted: S.
- Deleted: R.
- Deleted: D.
- Deleted: S.
- Deleted: T.
- Deleted: Deep Sea Research Part II: Topical Studies in Oceanography
- Deleted: ISSN: 0967-0645, Vol:
- Deleted: , Issue:
- Deleted: Page:
- Deleted: .
- Deleted: D
- Deleted:
- Deleted:

- Saba, G. K. and Steinberg, D. K.: Abundance, composition, and sinking rates of fish fecal pellets in the [Santa Barbara Channel](#), *Sci. Rep.*, 2, 1–6, doi:10.1038/srep00716, 2012.
- Siegel, D. A., Buesseler, K. O., Doney, S. C., Sailley, S. F., Behrenfeld, M. J. and Boyd, P. W.: [Global assessment of ocean carbon export by combining satellite observations and food-web models](#), *Global Biogeochem. Cycles*, 28, 181–196, doi:10.1002/2013GB004743, 2014.
- Stanley, R. H. R., Doney, S. C., Jenkins, W. J. and Lott, D. E.: Apparent oxygen utilization rates calculated from tritium and helium-3 profiles at the Bermuda Atlantic Time-series Study site, *Biogeosciences*, 9(6), 1969–1983, doi:10.5194/bg-9-1969-2012, 2012.
- Stukel, M.R., ~~Ohman, M. D.~~, ~~Benitez-Nelson, C. R.~~ and ~~Landry, M. R.~~: Contributions of mesozooplankton to vertical carbon export in a coastal upwelling system. *Mar Ecol Prog Ser.* 491, 47–65, doi: 10.3354/meps10453, 2013.
- Thunell, R. C.: Particle fluxes in a coastal upwelling zone: sediment trap results from Santa Barbara Basin, California, *Deep Sea Res. Part II Top. Stud. Oceanogr.*, 45(8), 1863–1884, doi:https://doi.org/10.1016/S0967-0645(98)80020-9, 1998.
- Yao, X. and Schlitzer, R.: Assimilating water column and satellite data for marine export production estimation, *Geosci. Model Dev.*, 6(5), 1575–1590, doi:10.5194/gmd-6-1575-2013, 2013.
- 15 Zaneveld, J. R. V., Variation of optical sea parameters with depth, in *Lecture Series on Optics of the sea*, 61, 2.3-1-2.3-22, 1973

Deleted: s

Deleted: b

Deleted: c

Deleted: Global Biogeochemical Cycles,

Moved down [7]: M. D.

Moved (insertion) [7]

Moved down [8]: C. R.

Moved (insertion) [8]

Moved down [9]: M. R.

Moved (insertion) [9]

Study Loc.	CFE	Latitude (°N)	Longitude (°W)	Dive	Bottle	Filter	UTC	UTC	Hours	Depth (m)	Depth stdev	Sample Notes	
							Day Start	Day End					
1	2	35.0739	121.1281	40	1	Supor	160.064	160.270	4.944	0.2		CFE-Cal did not dive	
1	2			41	2	QMA	160.333	160.500	4.008	70.0	12.3		
1	2			42	3	Supor	160.623	160.791	4.032	119.4	7.8	not analyzed	Deleted: anchovy fecal pellets
1	2	34.9978	121.1650	43	4	QMA*	160.849	160.851	0.048	186.0			Deleted: anchovy fecal pellets, not analyzed
1	4	35.0885	121.1293	40	1	QMA	160.076					selector failure	Deleted: sampler closed after bottle 4
1	4			41	2	Supor	160.297					selector failure	
1	4			42	3	QMA	160.422					selector failure	
1	4	35.0341	121.1862	43	4	Supor	160.732					selector failure	
1	2	34.9396	121.2031	50	1	QMA	162.091	162.294	4.872	131.7	10.9		
1	2			51	2	Supor	162.424	162.536	2.688	31.8	4.4	not analyzed	Deleted: sample not analyzed
1	2				3	QMA*							
1	2	34.8962	121.2032		4	Supor*							
1	4	34.9348	121.1946	50	1	Supor	162.075	162.280	4.908	189.5	7.7	oil under sample stage	Deleted: reticle
1	4			51	2	QMA	162.410	162.412	0.048	286.2		depth unstable	Deleted: , bottle 2 briefly
1	4			52	3	Supor	162.549	162.551	0.048			depth unstable	Deleted: e, bottle 3 briefly
1	4	34.8997	121.2165		4	QMA*							
2	2	34.7771	122.0572	60	1	Supor	165.047	165.264	5.208	142.9	3.8		
2	2			61	2	Supor	165.406	165.574	4.032	112.8	4.3		
2	2			62	3	Supor	165.716	165.883	4.008	97.7	4.1		
2	2	34.8651	122.3355		4	QMA	166.024	166.026	0.048			surfaced open at position 4	
2	4	34.7742	122.0587	60	1	QMA	165.060	165.278	5.232	160.9	4.2	C:N >20	
2	4			61	2	Supor	165.430	165.597	4.008	153.1	5.7	not analyzed	Deleted: not analyzed, large jelly (not imaged)
2	4			62	3	QMA	165.739	165.900	3.864	150.2	3.0		
2	4	34.8825	122.3499		4	Supor*							
2	2	34.7098	122.3004	70	1	Supor	166.659	166.882	5.352	159.2	5.1		
2	2			71	2	QMA	167.034	167.202	4.032	146.2	5.8		

2	2			72	3	Supor	167.350	167.517	4.008	147.8	3.9	
2	2	34.6771	122.4122		4	QMA*						
2	4	34.7091	122.2998	70	1	QMA	166.673	166.897	5.376	164.2	10.3	
2	4			71	2	Supor	167.044	167.211	4.008	157.6	3.4	
2	4			72	3	QMA	167.364	167.531	4.008	151.5	2.9	C:N >20
2	4	34.6829	122.4185		4	Supor*						
3	2	34.2275	123.1480	80	1	QMA	170.192	170.368	4.224	141.5	6.7	
3	2			81	2	Supor	170.472	170.639	4.008	131.4	3.8	
3	2			82	3	QMA	170.740	170.879	3.336	143.7	6.7	C:N >20
3	2	34.1717	123.0758		4	Supor*						
3	4	34.1129	122.9885	90	1	QMA	171.205	171.414	5.016	173.4	3.3	
3	4			91	2	Supor	171.553	171.721	4.032	160.9	0.1	
3	4			92	3	QMA	171.860	171.903	1.032	148.8	0.8	
3	4	34.0749	122.8673		4	Supor*						
3	2	34.1086	122.9823	90	1	Supor	171.190	171.369	4.296	126.9	4.8	
3	2			91	2	QMA	171.468	171.636	4.032	159.7	5.7	
3	2			92	3	Supor	171.737	171.904	4.008	154.7	3.6	
3	2	34.0714	122.8552		4	QMA*						
4	4	34.4070	123.0958	100	1	Supor	174.180	174.369	4.536	190.6	5.7	
4	4			101	2	Supor	174.489	174.657	4.032	117.3	3.3	
4	4			102	3	Supor	174.767	174.899	3.168	135.0	3.5	
4	4	34.4174	123.0535		4	Supor*						
4	2	34.4032	123.0964	100	1	QMA	174.294	174.354	1.440	165.8	132.5	depth unstable
4	2			101	2	Supor	174.479	174.646	4.008	139.9	3.0	
4	2			102	3	QMA	174.742	174.903	3.864	129.5		
4	2	34.4216	123.0310		4	Supor*						
4	4	34.4221	123.0133	110	1	QMA	175.187	175.487	7.200	164.0	5.4	
4	4			111	2	Supor	175.599	175.878	6.696	101.7	3.7	
4	4			112	3	QMA	175.989	176.267	6.672	158.6	3.9	

Deleted: didn't settle at depth

4	4	34.4449	123.0205	113	4	Supor	176.396	176.496	2.400	119.8	1.8	
4	2	34.4218	123.0168	110	1	Supor	175.173	175.469	7.104	162.8	5.5	
4	2			111	2	QMA	175.582	175.859	6.648	159.5	3.4	swimming siphonophore,
4	2			112	3	Supor	175.965	176.242	6.648	156.9	3.0	
4	2	34.4335	123.1008	113	4	Supor	176.350	176.516	3.984	153.1	2.3	

Deleted: jelly in sample, was imaged

Table 1: CFE-Cal 2017 deployments during the California Current Ecosystem Long Term Ecological Research process study

This table notes the location number, CFE number, longitude and latitude position, dive number, bottle number, filter type, sampling interval and depth interval of sampling. Filters marked with the * symbol are process blanks. The note column indicates any sample notes, including any instrument malfunctions.

5

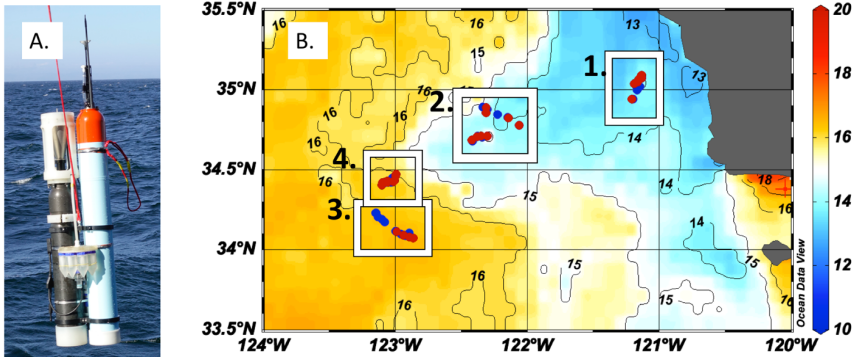


Figure 1: (A) CFE-Cal during deployment from R/V Revelle in 2017. The sampling system for particles is interfaced between the Optical Sedimentation Recorder (left) and SOLO float (right). (B) Map of CFE-Cal deployment and drift locations overlaying map of sea surface temperature (°C) for June 10-17 2017 from NASA Ocean Color Aqua Modis 4km resolution (<https://oceancolor.gsfc.nasa.gov/>). Blue dots within location boxes represent CFE-Cal 002 and red dots represent CFE-Cal 004 positions.

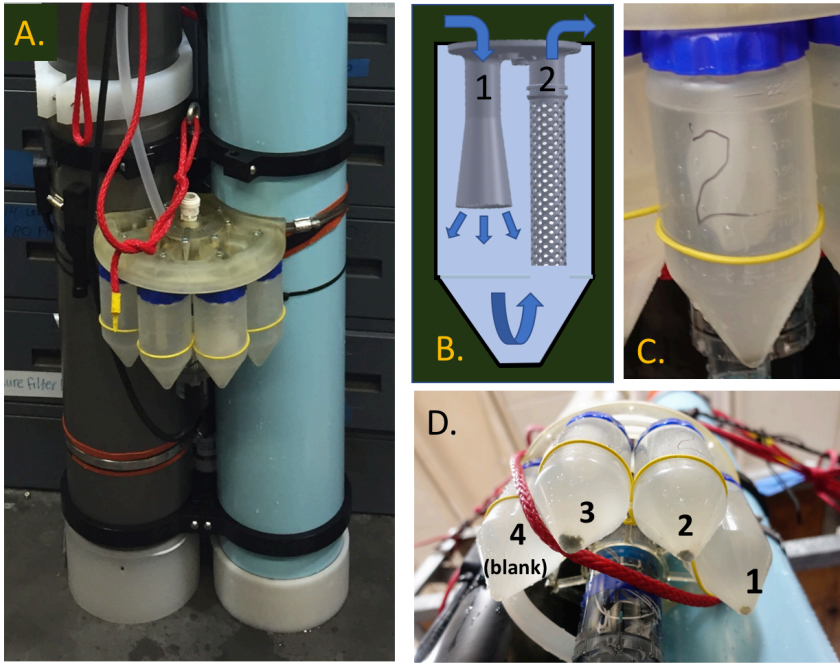
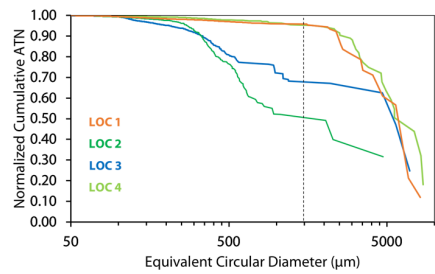
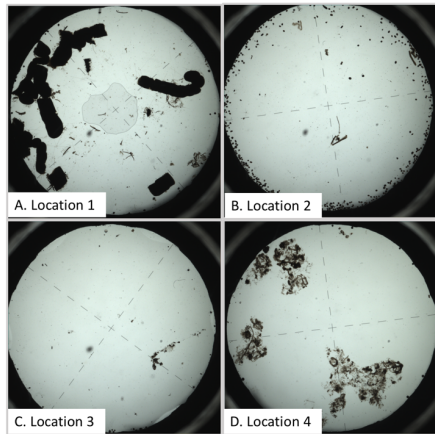


Figure 2: (A) Sampler on CFE-Cal. Suction action of a pump draws water and particles down a poly tube to the sampler (shown disconnected). (B) Detail of particle retention system within sample bottles. Inlet is cone shaped to decelerate incoming flow. Outlet is formed to accommodate 51 μm mesh which is retained by two o-rings at the top. (C) Closeup of bottle with Mesh filter in place; Filter area is $\sim 130 \text{ cm}^2$. (D) CFE-Cal recovery after 24-hour deployment showing collected samples. Bottle 2 is shown in C. In this case, bottle 4 was a blank (i.e. no particles directed to it).



5 **Figure 3: Representative images from four locations. The**
particle size classes present varied widely at the four different
locations. (A) In location 1, flux was dominated by large 1 mm
diameter anchovy fecal pellets. (B) Flux was dominated by
small ovoid pellets 200-300 microns in diameter. (C) Location 3
 10 **was characterized by very low flux. Flux was dominated by**
small particles with the occasional large aggregate. (D) Flux was
dominated by large aggregates. (E) cumulative normalized
volume attenuation vs. equivalent circular diameter curves
representative of the 4 locations. Approximately 95% of flux
 15 **was carried by aggregates >1.5 mm in size at locations 1 and 4.**
Location 2 had ~50% of flux in >1.5 mm fraction.

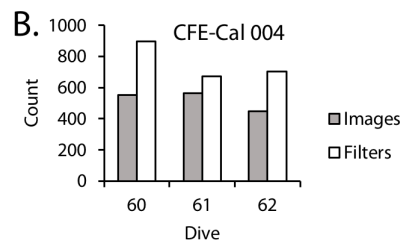
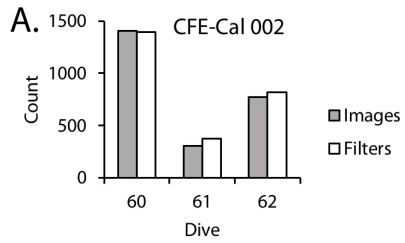


Figure 4: Comparison counts of ovoid pellets in images versus on filters. (A) CFE-CAL002 Deployment 3 (first deployment at location 2) (B) CFE-CAL004 Deployment 4 (second deployment at location 2).

5

Deleted: 2

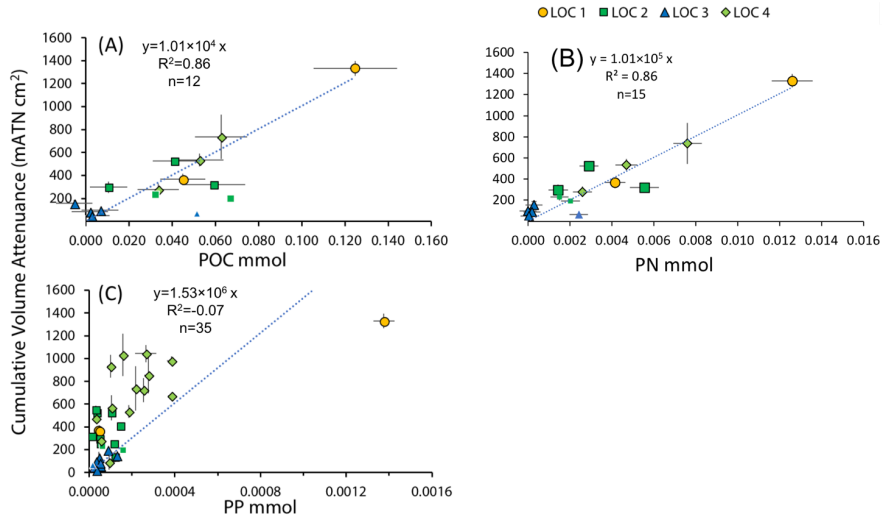
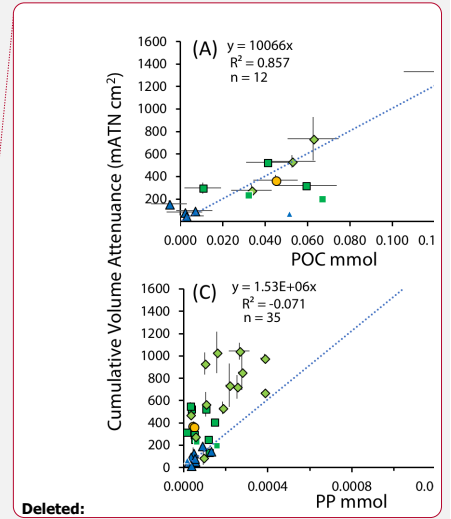


Figure 5: Data and regressions of sample POC (A), PN (B) and PP (C) vs. cumulative volume attenuation. Fits are forced through zero. Smaller symbols in all plots denote samples excluded from the POC regression analysis; these had C/N values >20 and were likely contaminated for carbon and not nitrogen. No data was excluded from PN or PP regressions.



Deleted:

Deleted: and D

Deleted: P regressions (C and D) include and exclude, respectively the high P enriched sample which was dominated by anchovy fecal pellets.

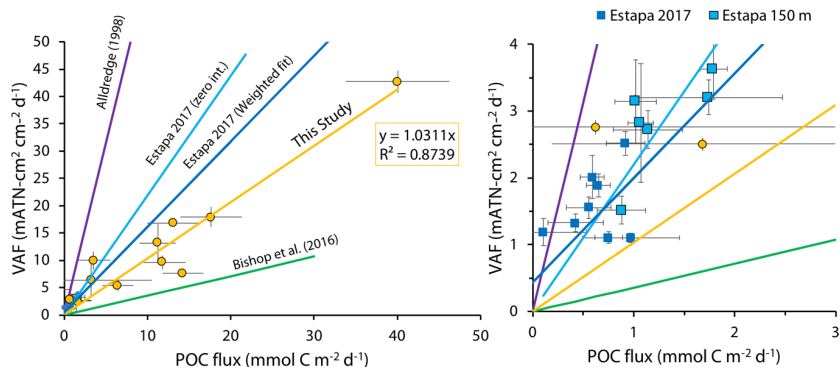


Figure 6:

Regressions of Volume Attenuance Flux ($\text{mATN-cm}^2 \text{cm}^{-2} \text{d}^{-1}$) to POC ($\text{mmol C m}^2 \text{d}^{-1}$) for this study (orange points and line: $y = 1.03x$, $R^2=0.874$), Estapa et al. (2017, dark blue, weighted fit: $y = 1.56x + 0.434$, $R^2 = 0.632$; light blue line, $y = 2.191x$, $R^2 = 0.47$), Bishop et al. 2016 estimated slope (green line) is $y=0.357x$ (1.0/2.8). Alldredge (1998) estimated slope (purple line) = $y=6.25x$. As this study's calibration is created using samples collected at 150m, we separate out Estapa's (2017) data points collected in 150m by marking them in light blue for comparison. (A) shows the entire range of VAF and POC flux from this study. (B) expanded graph near the origin ($x < 3 \text{ mmol C m}^{-2} \text{d}^{-1}$) showing the range of Estapa et al. (2017) data.

Deleted: ATN-POC

Formatted: Font: Not Italic, Font color: Text 1

Formatted: Font: Not Italic, Font color: Text 1

Formatted: Font: Not Italic, Font color: Text 1

Deleted:

Formatted: Font: Not Italic, Font color: Text 1

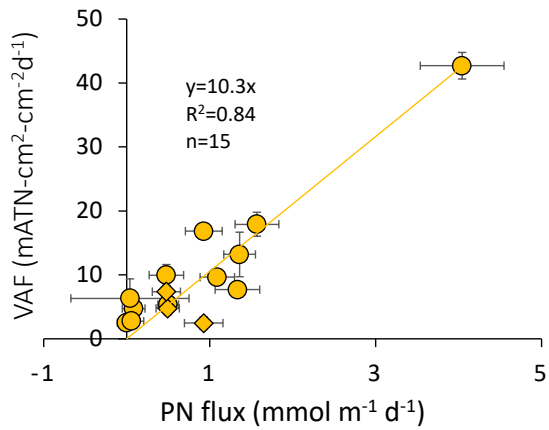


Figure 7:

Regressions of Volume Attenuance Flux (mATN-cm² cm² d⁻¹) to PN (mmol N m² d⁻¹)

5

Deleted: Provide a figure caption here.

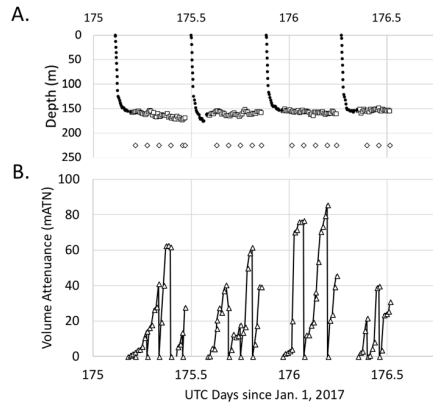
Formatted: Normal, Right: 0", Line spacing: single

Formatted: Font: Not Italic, Font color: Text 1, English (UK)

Deleted: Regressions of ATN-POC (mATN-cm² cm² d⁻¹) to POC (mmol C m² d⁻¹) for this study (orange: $y = 1.03x$, $R^2 = 0.874$), Estapa et al. (2017, blue, $y = 1.56x + 0.434$, $R^2 = 0.632$; light blue, $y = 2.191x$, $R^2 = 0.47$). Bishop et al. 2016 estimated slope (green) is 0.357 (1.0/2.8). Alldredge (1998) estimated slope (purple) = 6.25.

Deleted:Page Break.....

Appendix Figures.



5 **Figure A1: (a) Typical deployment trajectory of a CFE-Cal. This**
particular deployment is from CFE2, the first deployment at
location 4. The x-axis is time in days (Jan 1 2017 at 1200UTC =
day 0.5). The filled black circles are depths as the CFE-Cal is
diving, open black squares denote depths as the CFE drifts and
takes images of settled particles. The open black diamonds
represent times when the sample stage was cleaned and particles
directed into a sample bottle. (b) Graph B shows the
corresponding attenuation for each photo taken. Particles build-
up over time and then periodically the glass stage will be rinsed
off and particles directed into the sample bottles. Due to a
programming error, the sampler and particles are not removed
from the stage.

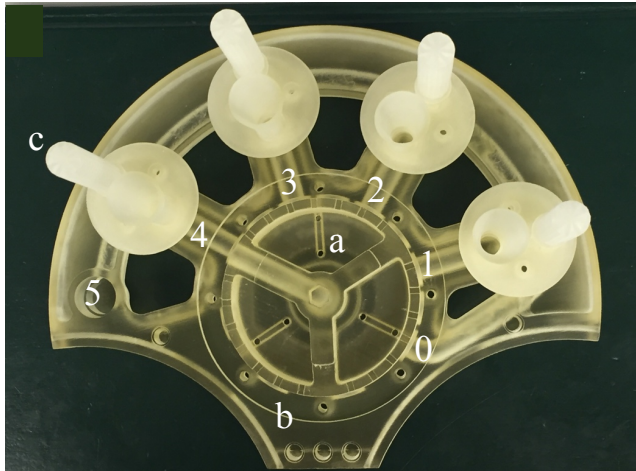


Figure A3: Sampler elements: (a) sample selector rotator; (b) main structural element of the sampler. Flow paths (1-4) direct water and particles into sample bottles or (0) to bypass sample bottles; and (c) particle retention system which bridges inflow channels and common exhaust manifold channel (5). Sample rotator is shown open at position 4. When not sampling, the rotator is sealed to closed positions.

5

10

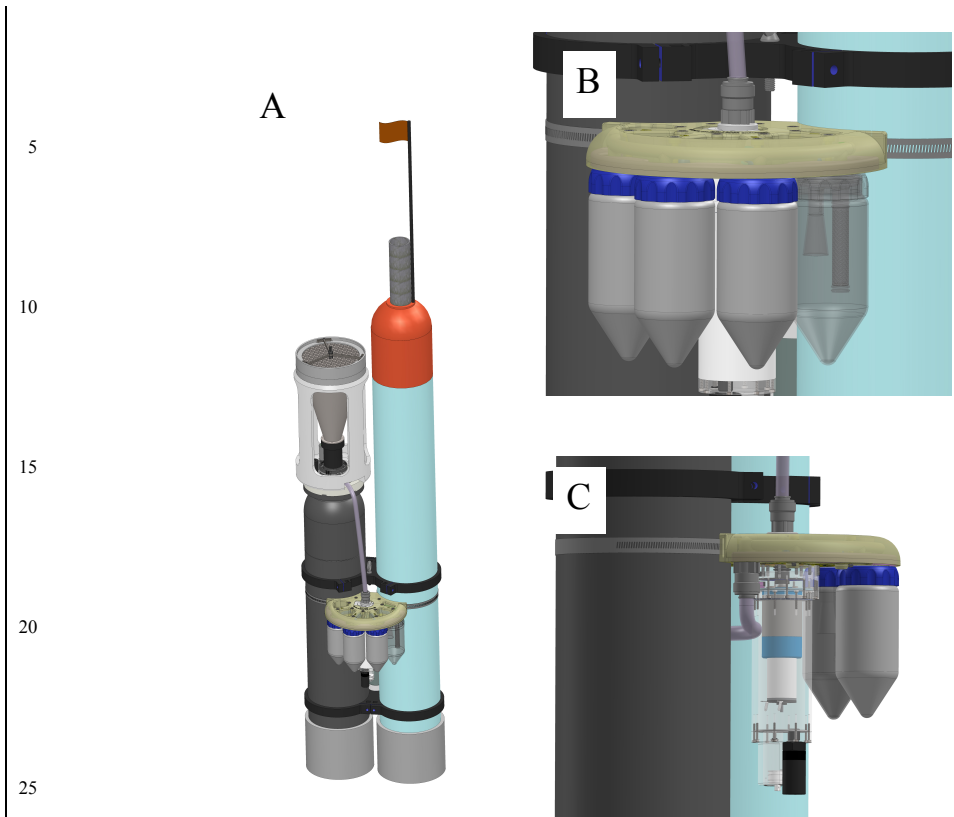
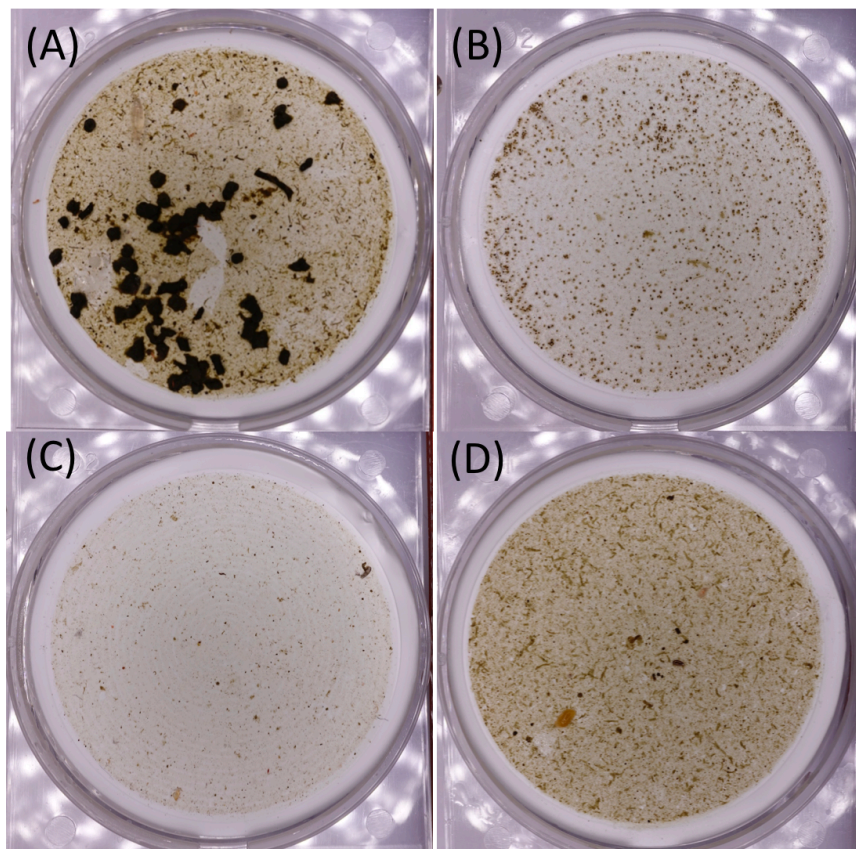


Figure A4: CFE-Cal configuration. (a) CFE-Cal configuration (b) Close up of attached sampling system. Far right bottle translucent to show details of bottle inlet and outlet. (c) Side view of sampler with one of the bottles removed to show how motor housing is attached to the sampler.

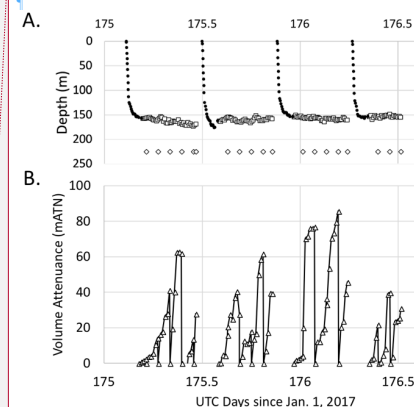
35



5 **Figure A5: Representative images of sampled particulates from locations 1-4. The process of sampling retains morphology of cohesive aggregates and. Turbulence on transit from imaging stage to bottle does disrupt the integrity of loosely aggregated millimeter sized particles such as represented in Figure 3D. (a) Location 1. CFE 002 dive 42 - Days 160.623 to 160.791 - Depth 119.4 ± 7.8 m. (b) Location 2. CFE 004 dive 71 - Days 167.034 to 167.202 - Depth 157.6 ± 3.4 m. (c) CFE 002 dive 90 - Days 171.190 171.369 - Depth 126.9 ± 4.8 m. (d). Location 4. CFE 002 dive 101 - Days 174.479 to 174.646 - Depth 139.9 ± 3.0 m.**

Deleted:Page Break.....

Appendix Figures.



ADD TILT FIGURE HERE

Figure A1: (a) Typical deployment trajectory of a CFE-Cal. The x-axis is time in days (Jan 1 2017 at 1200UTC = day 0.5). The filled black circles are depths as the CFE-Cal is diving, open black squares denote depths as the CFE drifts and takes images of settled particles. The open black diamonds represent times when the sample stage was cleaned and particles directed into a sample bottle. (b) Graph B shows the corresponding attenuation for each photo taken. Particles build-up over time and then periodically the glass stage will be rinsed off and particles directed into the sample bottles. Due to a programming error, the sampler and particles are not removed from the stage.

.....Page Break.....

<object><object>

.....Page Break.....

<object>

Figure A3: Representative images of sampled particulates from locations 1-4. The process of sampling retains morphology of cohesive aggregates and. Turbulence on transit from imaging stage to bottle does disrupt the integrity of loosely aggregated millimeter sized particles such as represented in Figure 3D. (a) Location 1. CFE 002 dive 42 - Days 160.623 to 160.791 - Depth 119.4 ± 7.8 m. (b) Location 2. CFE 004 dive 71 - Days 167.034 to 167.202 - Depth 157.6 ± 3.4 m. (c) CFE 002 dive 90 - Days 171.190 171.369 - Depth 126.9 ± 4.8 m. (d). Location 4. CFE 002 dive 101 - Days 174.479 to 174.646 - Depth 139.9 ± 3.0 m.

Formatted: Normal

Formatted: Font: Not Italic, Font color: Text 1

Page 9: [1] Deleted **Hannah Bourne** **12/21/18 3:23:00 PM**



Page 11: [2] Deleted **Jim Bishop** **12/19/18 2:53:00 PM**



Page 11: [2] Deleted **Jim Bishop** **12/19/18 2:53:00 PM**



Page 11: [2] Deleted **Jim Bishop** **12/19/18 2:53:00 PM**



Page 11: [2] Deleted **Jim Bishop** **12/19/18 2:53:00 PM**



Page 11: [3] Deleted **Jim Bishop** **12/19/18 2:50:00 PM**



Page 11: [3] Deleted **Jim Bishop** **12/19/18 2:50:00 PM**



Page 11: [4] Deleted **Hannah Bourne** **11/23/18 5:53:00 PM**



Page 11: [5] Deleted **Jim Bishop** **12/19/18 3:08:00 PM**



Page 11: [5] Deleted **Jim Bishop** **12/19/18 3:08:00 PM**



Page 11: [5] Deleted **Jim Bishop** **12/19/18 3:08:00 PM**



Page 11: [5] Deleted **Jim Bishop** **12/19/18 3:08:00 PM**



Page 11: [6] Deleted **Jim Bishop** **12/19/18 3:08:00 PM**



Page 11: [7] Deleted **Jim Bishop** **12/19/18 3:00:00 PM**



Page 11: [8] Formatted	Hannah Bourne	11/23/18 12:22:00 PM
-------------------------------	----------------------	-----------------------------

Font: Not Italic, Font color: Text 1

Page 11: [8] Formatted	Hannah Bourne	11/23/18 12:22:00 PM
-------------------------------	----------------------	-----------------------------

Font: Not Italic, Font color: Text 1

Page 11: [9] Formatted	Hannah Bourne	11/23/18 12:22:00 PM
-------------------------------	----------------------	-----------------------------

Font: Not Italic, Font color: Text 1

Page 11: [9] Formatted	Hannah Bourne	11/23/18 12:22:00 PM
-------------------------------	----------------------	-----------------------------

Font: Not Italic, Font color: Text 1

Page 11: [10] Deleted	Hannah Bourne	12/21/18 10:40:00 AM
------------------------------	----------------------	-----------------------------

Page 11: [11] Deleted	Jim Bishop	12/19/18 3:53:00 PM
------------------------------	-------------------	----------------------------

Page 11: [11] Deleted	Jim Bishop	12/19/18 3:53:00 PM
------------------------------	-------------------	----------------------------

Page 11: [11] Deleted	Jim Bishop	12/19/18 3:53:00 PM
------------------------------	-------------------	----------------------------

Page 11: [11] Deleted	Jim Bishop	12/19/18 3:53:00 PM
------------------------------	-------------------	----------------------------